

Article

Reliability Analysis and Applications of Generalized Type-II Progressively Hybrid Maxwell–Boltzmann Censored Data

Ahmed Elshahhat ^{1,*} , Osama E. Abo-Kasem ² and Heba S. Mohammed ³¹ Faculty of Technology and Development, Zagazig University, Zagazig 44519, Egypt² Department of Statistics, Faculty of Commerce, Zagazig University, Zagazig 44519, Egypt; o.e.abokasem@zu.edu.eg³ Department of Mathematical Sciences, College of Science, Princess Nourah bint Abdulrahman University, P.O. Box 84428, Riyadh 11671, Saudi Arabia; hsmohammed@pnu.edu.sa

* Correspondence: aelshahhat@ftd.zu.edu.eg

Abstract: Today, the reliability or quality practitioner always aims to shorten testing duration and reduce testing costs without neglecting efficient statistical inference. So, a generalized progressively Type-II hybrid censored mechanism has been developed in which the experimenter prepays for usage of the testing facility for T units of time. This paper investigates the issue of estimating the model parameter, reliability, and hazard rate functions of the Maxwell–Boltzmann distribution in the presence of generalized progressive Type-II hybrid censored data by making use of the likelihood and Bayesian inferential methods. Using an inverse gamma prior distribution, the Bayes estimators of the same unknown parameters with respect to the most commonly squared-error loss are derived. Since the joint likelihood function is produced in complex form, following the Monte-Carlo Markov-chain idea, the Bayes' point estimators as well as the Bayes credible and highest posterior density intervals cannot be derived analytically, but they may be examined numerically. Via the normal approximation of the acquired maximum likelihood and log-maximum-likelihood estimators, the approximate confidence interval bounds of the unknown quantities are derived. Via comprehensive numerical comparisons, with regard to simulated root mean squared-error, mean relative absolute bias, average confidence length, and coverage probability, the actual behavior of the proposed estimation methodologies is examined. To illustrate how the offered methodologies may be used in real circumstances, two different applications, representing the failure time points of aircraft windscreens as well as the daily average wind speed in Cairo during 2009, are explored. Numerical evaluations recommend utilizing a Bayes model via the Metropolis-Hastings technique to produce samples from the posterior distribution to estimate any parameter of the Maxwell–Boltzmann distribution when collecting data from a generalized progressively Type-II hybrid censored mechanism.

Keywords: Maxwell–Boltzmann model; Bayes inference; maximum likelihood; reliability analysis; Monte-Carlo Markov-chain algorithms; generalized Type-II progressive hybrid censoring

MSC: 62F10; 62F15; 62N01; 62N02; 62N05



Citation: Elshahhat, A.; Abo-Kasem, O.E.; Mohammed, H.S. Reliability Analysis and Applications of Generalized Type-II Progressively Hybrid Maxwell–Boltzmann Censored Data. *Axioms* **2023**, *12*, 618. <https://doi.org/10.3390/axioms12070618>

Academic Editor: Lechang Yang, Qingqing Zhai, Rui Peng and Aibo Zhang

Received: 30 May 2023

Revised: 19 June 2023

Accepted: 20 June 2023

Published: 21 June 2023



Copyright: © 2023 by the authors. Licensee MDPI, Basel, Switzerland. This article is an open access article distributed under the terms and conditions of the Creative Commons Attribution (CC BY) license (<https://creativecommons.org/licenses/by/4.0/>).

1. Methodology and Materials

This section includes three subsections: the first presents the formal presentation of the proposed strategy; the second presents the formal presentation of the proposed model; and the last is devoted to study contributions.

1.1. Generalized Type-II Progressive Hybrid Censoring

If the lifespan of certain objects is quite long and/or the sample size n is extreme, it is difficult to continue the test until all n observations are made (full data). To end the test under predetermined conditions, there is a more cost-effective strategy called the

censored mechanism. For background information on reliability and safety customization techniques, readers may refer to BahooToroody et al. [1] and Falcone et al. [2].

Progressive Type-II censoring (T2PC), discussed in detail by Balakrishnan and Cramer [3], has gotten a lot of interest since it permits surviving individuals to be removed from a study at various points other than the end point. Though, if the experimental subjects are extremely reliable, it may take longer to perform the test. Thus, to improve the T2PC strategy, Type-I progressive hybrid censoring (T1PHC) was presented by Kundu and Joarder [4]. On the other hand, T1PHC has the drawback of having very few failures that can occur before time T , which means that the offered maximum likelihood estimators (MLEs) cannot always be evaluated. So, Type-II progressive hybrid censoring (T2PHC) was proposed by Childs et al. [5]. Although the T2PHC assures an efficient amount of visible failures, collecting the required failures may take a bit of time.

As a result, Type-II generalized progressive hybrid censoring (T2GPHC) was introduced by Lee et al. [6]. To perform the T2GPHC process, follow these steps:

1. Specify the total experimental items n , number of failures m , two thresholds T_i , $i = 1, 2$ (where $0 < T_1 < T_2 < \infty$) and the progressive censoring $R = (R_1, R_2, \dots, R_m)$ (where $n (= \sum_{i=1}^m R_i + m)$).
2. Determine the total number of failures $d_1 (< d_2)$ up to $T_1 (< T_2)$.
3. Start the experiment by placing n independent and identical items into a test.
4. When the first failure item (say $X_{1:m:n}$) is recorded, R_1 of the surviving items (out of $n - 1$ units) are randomly selected and withdrawn from the experiment. Next, when the second failure item (say $X_{2:m:n}$) is recorded, R_2 of the surviving items (out of $n - 2 - R_1$ units) are randomly selected and withdrawn from the experiment, and so on.
5. Stop the experiment at time $\mathcal{T}^\circ = \max\{T_1, \min\{X_{m:m:n}, T_2\}\}$.
6. If $X_{m:n} < T_1$, set $R_i = 0$, $i = m, m + 1, \dots, d_1$, the experiment continues until it stops at T_1 (referred to as Case-I).
7. If $T_1 < X_{m:m:n} < T_2$, the experiment stops at $X_{m:m:n}$ (referred to as Case-II).
8. If $T_2 < X_{m:m:n}$, the experiment stops at T_2 (referred to as Case-III).

Subsequently, the researcher will collect one of the following three data sets of observations:

$$\{\underline{X}, \mathbf{R}\} = \begin{cases} \{(X_{1:m:n}, R_1), \dots, (X_{m-1:m:n}, R_{m-1}), (X_{m:m:n}, 0), \dots, (X_{d_1:n}, 0)\}; & \text{Case-I,} \\ \{(X_{1:m:n}, R_1), \dots, (X_{d_1:n}, R_{d_1}), \dots, (X_{m-1:m:n}, R_{m-1}), (X_{m:m:n}, R_m)\}; & \text{Case-II,} \\ \{(X_{1:m:n}, R_1), \dots, (X_{d_1:n}, R_{d_1}), \dots, (X_{d_2-1:n}, R_{d_2-1}), (X_{d_2:n}, R_{d_2})\}; & \text{Case-III.} \end{cases}$$

It is critical to remember that the T2GPHC modifies the T2PHC by guaranteeing that the test is completed at T_2 . Thus, this threshold is the longest duration that the examiner endures to allow the study to run. Moreover, T2GPHC can be considered a new extension of several control strategies that can be obtained as sub-plans, such as:

- T1PHC, by Kundu and Joarder [4], if $T_1 \rightarrow 0$.
- T2PHC, by Childs et al. [5], if $T_2 \rightarrow \infty$.
- Type-I Hybrid, by Epstein [7], if $T_1 \rightarrow 0$, $R_j = 0$, for $j = 1, 2, \dots, m - 1$, and $R_m = n - m$.
- Type-I Hybrid, by Childs et al. [8], if $T_2 \rightarrow \infty$, $R_j = 0$, for $j = 1, 2, \dots, m - 1$, and $R_m = n - m$.
- Type-I censoring, by Bain and Engelhardt [9], if $T_1 = 0$, $m = n$, $R_j = 0$, for $j = 1, 2, \dots, m - 1$, and $R_m = n - m$.
- Type-II censoring, by Bain and Engelhardt [9], if $T_1 = 0$, $T_2 \rightarrow \infty$, $R_j = 0$, for $j = 1, 2, \dots, m - 1$, and $R_m = n - m$.

However, let $\{X, R\}$ be a T2GPHC sample of size d_2 collected from a continuous distribution with cumulative distribution function (CDF) $F(\cdot)$ and probability density function (PDF) $f(\cdot)$. Then, the joint likelihood function (say $L_c(\cdot)$) of the observed T2GPHC data, for $\tau = 1, 2$, can be formulated as

$$L_c(\sigma|X) = \mathcal{K}_c \mathcal{R}_c(T_\tau; \sigma) \prod_{j=1}^{J_c} f(x_{i:m:n}; \sigma) [1 - F(x_{i:m:n}; \sigma)]^{R_j}, \tag{1}$$

where Case-I, Case-II, and Case-III denoted by $c = 1, 2, 3$ correspondingly, and $\mathcal{R}_c(\cdot)$ is a combined-term of reliability functions at $T_i, i = 1, 2$ points. Table 1 displays the T2GPHC's notations.

Table 1. Notations of the T2GPHC process.

c	\mathcal{K}_c	J_c	$\mathcal{R}_c(T_\tau; \sigma)$	$R_{d_\tau+1}^*$
I	$\prod_{j=1}^{d_1} \sum_{i=j}^m (R_i + 1)$	d_1	$[1 - F(T_1; \sigma)]^{R_{d_1+1}^*}$	$n - d_1 - \sum_{i=1}^{m-1} R_i$
II	$\prod_{j=1}^m \sum_{i=j}^m (R_i + 1)$	m	1	0
III	$\prod_{j=1}^{d_2} \sum_{i=j}^m (R_i + 1)$	d_2	$[1 - F(T_2; \sigma)]^{R_{d_2+1}^*}$	$n - d_2 - \sum_{i=1}^{d_2} R_i$

In recent years, using the T2GPHC mechanism, several studies have proposed different estimates for various statistical parameters of life. For example; see Ashour and Elshahhat [10], Ateya and Mohammed [11], Seo [12], Cho and Lee [13], Wang et al. [14], Nagy et al. [15], Alotaibi et al. [16], Elshahhat et al. [17,18], and references cited therein.

1.2. Maxwell–Boltzmann Model

In the second half of the 1800s, James Clerk Maxwell and Ludwig Boltzmann found out the distribution of speeds in a gas at a specific temperature. Their finding is referred to as the Maxwell-Boltzmann (MB(σ)) distribution since it illustrates how the speeds of molecules are spread for an ideal gas. It also serves as the foundation for gas kinetic energy, which explains many fundamental phenomena of gases such as pressure and diffusion. Since the MB distribution function provides the most probable speed, the average speed, and the root-mean-square speed that may be determined, it has a wide range of applications in physical, chemical, statistical mechanics, and reliability analysis. For additional details, see Peckham and McNaught [19] and Rowlinson [20]. Suppose X is a random variable of lifetime that follows the MB(σ) distribution, where $\sigma > 0$ is the scale parameter, then its PDF and CDF, are provided by

$$f(x; \sigma) = \frac{4}{\sqrt{\pi}} \frac{x^2}{\sqrt{\sigma^3}} e^{-\frac{x^2}{\sigma}}, \quad x > 0, \tag{2}$$

and

$$F(x; \sigma) = \Gamma_{\frac{3}{2}} \left(\frac{x^2}{\sigma} \right), \tag{3}$$

respectively, where $\Gamma_a(\beta) = \frac{1}{\Gamma(a)} \int_0^\beta y^{a-1} e^{-y} dy$ (is known as gamma function) and $\Gamma(a) = \int_0^\infty y^{a-1} e^{-y} dy$ (is known as an incomplete-gamma function). The equivalent form of the function (3) takes the following expression

$$\begin{aligned} F(x; \sigma) &= 2\text{erf} \left(\frac{x}{\sqrt{\sigma}} \right) - \frac{2}{\sqrt{\pi}} \frac{x}{\sqrt{\sigma}} e^{-\frac{x^2}{\sigma}}, \\ &= 1 - \frac{4}{\sqrt{\pi}} \frac{1}{\sqrt{\sigma^3}} \xi(x, 2, \sigma), \end{aligned} \tag{4}$$

where $\text{erf}(x) = \frac{2}{\sqrt{\pi}} \int_0^x e^{-y^2} dy$ is the error term and $\zeta(x, \alpha, \sigma) = \int_x^\infty y^\alpha e^{-\frac{y^2}{\sigma}} dy$. From now on, the CDF (4) will be used wherever it is requested.

Moreover, we consider two unknown time parameters, namely: reliability function (RF) $R(\cdot)$ and hazard rate function (HRF) $h(\cdot)$ of the MB distribution, at distinct time $t > 0$, are given by

$$R(t; \sigma) = \frac{4}{\sqrt{\pi}} \frac{1}{\sqrt{\sigma^3}} \zeta(t, 2, \sigma), \quad (5)$$

and

$$h(t; \sigma) = t^2 e^{-\frac{t^2}{\sigma}} \zeta^{-1}(t, 2, \sigma). \quad (6)$$

From (2), Bekker and Roux [21] stated that the MB model is a particular member of the generalized Weibull and generalized Rayleigh distributions. Also, Krishna and Malik [22] showed that the MB failure rate (6) belongs to the group of increasing HRF distributions. So, it possesses all of the desirable characteristics that make it highly valuable in life-testing and reliability studies, particularly in cases where the assumption of a constant failure rate is unrealistic. In reliability literature during the last decade, the MB distribution has become a popular model and has been extensively studied in reliability theory by many authors, for example, Krishna and Malik [22,23] considered the conventional Type-II censored and T2PC data, respectively; Krishna et al. [24] developed randomly censored data; Tomer and Panwar [25] studied T1PHC data; Chaudhary and Tomer [26] addressed the stress–strength of T2PC data; later, Pathak et al. [27] considered the T2PC with binomial removals for the step-stress partially accelerated data, among many other works.

1.3. Study Objectives

Although these research efforts offer a reliability treatment for the MB distribution in the presence of various reliability scenarios, they lack light on the MB's applicability characteristics, particularly in the presence of data collected from the proposed T2GPHC strategy. To achieve this goal, using the T2GPHC strategy, the main contribution of the current study is fourfold:

1. Develop maximum likelihood estimators (MLEs) and Bayesian estimators (BE) for σ , $R(t)$ and $h(t)$.
2. Use the inverted gamma distribution and squared-error loss functions for deriving Bayes' estimates.
3. Employ the Markov-Chain Monte Carlo (MCMC) approximation paradigm to evaluate the nonlinear posterior function.
4. Construct approximate confidence interval (ACI) estimators for σ , $R(t)$ and $h(t)$, based on two different methods of asymptotic normality approximation.
5. Obtain Bayes credible interval (BCI) and highest posterior density (HPD) interval estimators from the MCMC variates.
6. Conduct an extensive evaluation of the estimates for σ , $R(t)$ and $h(t)$, based on four metrics: root mean squared errors, mean relative absolute biases, average confidence lengths, and coverage percentages.
7. Utilize three specific programming packages in the R 4.2.2 environment, namely: (1) 'coda' (by Plummer et al. [28]), (2) 'VGAM' (by Yee [29]), and (3) 'maxLik' (by Henningsen and Toomet [30]).
8. Apply the developed methodologies to two real-world data sets from the engineering and physics sectors, thereby demonstrating the applicability and versatility of the MB model. The data sets represent failure times of aircraft windshields and the daily average wind speed in Cairo city.

The rest of the article is organized as follows: In Sections 2 and 3, the acquired MLEs and BEs of σ , $R(t)$ and $h(t)$ are provided, respectively. Different intervals of σ , $R(t)$ and $h(t)$ are created in Section 4. Section 5 presents the Monte Carlo outcomes. In Section 6, real applications are analyzed. Ultimately, Section 7 reports the paper's conclusions.

2. Likelihood Inference

Suppose $\underline{X} = \{(X_{1:m:n}, R_1), \dots, (X_{d_1:n}, R_{d_1}), \dots, (X_{d_2:n}, R_{d_2})\}$ is a T2GPHC sample of size d_2 obtained from MB(σ). Inserting (2) and (3) into (1), where x_i is used in place of $x_{i:m:n}$ for simplicity in notation, then the likelihood function of σ in the presence of \underline{X} observations can be written as

$$L_c(\sigma|\underline{X}) \propto \sigma^{-\frac{3n}{2}} e^{-\sum_{i=1}^{J_c} \frac{x_i^2}{\sigma}} \zeta_c(T_\tau, 2, \sigma) \prod_{i=1}^{J_c} (\zeta(x_i, 2, \sigma))^{R_i}, \tag{7}$$

where $\zeta_i(T_i, 2, \sigma) = \int_{T_i}^{\infty} y^2 e^{-\frac{y^2}{\sigma}} dy$ for $i = 1, 2$, and $\zeta_2(T_\tau, 2, \sigma) = 0$.

Differentiating (7) in regard to σ , the MLE $\hat{\sigma}$ of σ can be owned by solving the next nonlinear normal equation:

$$\frac{1}{\sigma} \left[\frac{1}{\sigma} \sum_{i=1}^{J_c} x_i^2 - \frac{3}{2}n \right] + \frac{1}{\sigma^2} \left[\frac{\zeta_c(T_\tau, 4, \sigma)}{\zeta_c(T_\tau, 2, \sigma)} + \sum_{i=1}^{J_c} R_i \frac{\zeta(x_i, 4, \sigma)}{\zeta(x_i, 2, \sigma)} \right] \Bigg|_{\sigma=\hat{\sigma}} = 0. \tag{8}$$

It is obvious that, from (8), the solution of $\hat{\sigma}$ can be derived by a suitable iterative approach like the Newton-Raphson (NR) technique. Therefore, as soon as a given T2GPHC data set is available, we recommend applying the ‘maxLik’ package (which utilizes the NR function via maxNR(\cdot) command) to evaluate the acquired MLE $\hat{\sigma}$.

Next, once $\hat{\sigma}$ is evaluated, using the invariance feature of the MLE $\hat{\sigma}$, the MLEs $\hat{R}(t)$ and $\hat{h}(t)$ of $R(t)$ and $h(t)$ from (5) and (6), respectively, at mission time t can be easily acquired as

$$\hat{R}(t) = \frac{4}{\sqrt{\pi}} \frac{1}{\sqrt{\hat{\sigma}^3}} \zeta(t, 2, \hat{\sigma}) \quad \text{and} \quad \hat{h}(t) = t^2 e^{-\frac{t^2}{\hat{\sigma}}} \zeta^{-1}(t, 2, \hat{\sigma}), \tag{9}$$

respectively.

3. Bayes Inference

In Bayes’ estimation, we provide the prior information by running an experiment, and estimators are built to make inferences about the features of interest based on this updated knowledge. Because it offers legitimate alternatives to standard methodologies, this strategy has grown in popularity for analyzing failure data. This section introduces the BEs of σ , $R(t)$ and $h(t)$ of the MB model when a data set is obtained from the T2GPHC mechanism. First, according to Bekker and Roux [21], we assume that σ is a random variable with an inverted gamma (IG) density (symbolized by $\omega(\cdot)$) as

$$\omega(\sigma; a, b) \propto \sigma^{-(a+1)} e^{-b/\sigma}, \quad \sigma > 0, \tag{10}$$

where $a > 0$ and $b > 0$ are known. The IG distribution is useful as a prior for positive parameters. It imparts a quite heavy tail and keeps probability further from zero than the gamma distribution. It also offers different shapes depending on its parameter values and expresses the posterior distribution in a simple form. It should be noted that one can easily incorporate other conjugate density priors such as gamma, normal-inverse-gamma, and inverse gamma-gamma, among others.

Combining the prior (10) and likelihood (7) into the continuous Bayes’ theorem, the posterior distribution (say $\Omega(\cdot)$) of σ becomes

$$\Omega_c(\sigma|\underline{X}) = \mathcal{H}^{-1} \sigma^{-(\frac{3n}{2}+a+1)} e^{-\frac{1}{\sigma}(\sum_{i=1}^{J_c} x_i^2 + b)} \zeta_c(T_\tau, 2, \sigma) \prod_{i=1}^{J_c} (\zeta(x_i, 2, \sigma))^{R_i}, \tag{11}$$

where

$$\mathcal{H} = \int_0^\infty \sigma^{-\left(\frac{3n}{2}+a+1\right)} e^{-\frac{1}{\sigma}\left(\sum_{i=1}^Jc x_i^2+b\right)} \zeta_c(T_\tau, 2, \sigma) \prod_{i=1}^J (\zeta(x_i, 2, \sigma))^{R_i} d\sigma.$$

A loss function is significant in Bayes' approach since it may discover overestimation and underestimation in the study. In reliability analysis, the squared-error loss (SEL) function is suitable when decisions become increasingly damaging due to higher errors. Using this loss, the BE (say $\tilde{\sigma}$) of σ is developed by the posterior-expectation as:

$$\tilde{\sigma} = \mathcal{H}^{-1} \int_0^\infty \sigma \Omega_c(\sigma|X) d\sigma. \tag{12}$$

It is obvious, from (12), that the explicit solution of $\tilde{\sigma}$ is not possible. However, to draw a posterior sample of σ from (12), the Metropolis-Hastings (M-H) algorithm is adopted, for further detail, see Gelman et al. [31] and Lynch [32]. We, thus, evaluate the BEs of σ , $R(t)$ and $h(t)$ by 'coda' package (which utilizes the Metropolis-Hastings algorithm via `run_metropolis_MCMC(·)` command). Using the normal distribution as a proposal, do the following M-H steps:

Step-1: Set $\sigma^{(0)} = \hat{\sigma}$.

Step-2: Set $l = 1$.

Step-3: Obtain a candidate variate σ^* from normal $N(\hat{\sigma}, \widehat{var}(\hat{\sigma}))$ distribution.

Step-4: Obtain a candidate variate u^* from uniform $U(0, 1)$ distribution.

Step-5: Obtain $\mathcal{G} = \frac{\Omega_c(\sigma^*|X)}{\Omega_c(\sigma^{l-1}|X)}$.

Step-6: Set $\sigma^{(l)} = \sigma^*$ if $u^* \leq \min\{1, \mathcal{G}\}$, else set $\sigma^{(l)} = \sigma^{(l-1)}$.

Step-7: Evaluate the reliability $R(t)$ and hazard rate $h(t)$ parameters, at $t > 0$, as

$$R(t) = \frac{4}{\sqrt{\pi}} \frac{1}{\sqrt{\sigma^{(l)}^3}} \zeta(t, 2, \sigma^{(l)}) \quad \text{and} \quad h(t) = t^2 e^{-\frac{t^2}{\sigma^{(l)}}} \zeta^{-1}(t, 2, \sigma^{(l)}),$$

respectively.

Step-8: Set $l = l + 1$.

Step-9: Redo Steps 3-8 \mathcal{D} times, then ignore the first \mathcal{D}^\bullet iterations as burn-in, to get $\sigma^{(l)}$, $R^{(l)}(t)$ and $h^{(l)}(t)$ for $l = \mathcal{D}^\bullet + 1, \mathcal{D}^\bullet + 2, \dots, \mathcal{D}$.

Step-10: Get the BEs of σ , $R(t)$ and $h(t)$ as

$$\tilde{\sigma} = \frac{1}{\bar{\mathcal{D}}} \sum_{l=\mathcal{D}^\bullet+1}^{\mathcal{D}} \sigma^{(l)}, \quad \tilde{R}(t) = \frac{1}{\bar{\mathcal{D}}} \sum_{l=\mathcal{D}^\bullet+1}^{\mathcal{D}} R^{(l)}(t), \quad \text{and} \quad \tilde{h}(t) = \frac{1}{\bar{\mathcal{D}}} \sum_{l=\mathcal{D}^\bullet+1}^{\mathcal{D}} h^{(l)}(t),$$

respectively, where $\bar{\mathcal{D}} = \mathcal{D} - \mathcal{D}^\bullet$.

4. Interval Inference

In this section, the asymptotic (including: ACI-NA/ACI-NL) intervals based on the observed Fisher information as well as the Bayes (including: BCI/HPD) intervals based on the MCMC variates of σ , $R(t)$ or $h(t)$ are created.

4.1. Asymptotic Intervals

To build the $100(1 - q)\%$ ACI-NA (or ACI-NL) of σ , $R(t)$, or $h(t)$, the associated asymptotic normality of their MLEs is used. Using the observed Fisher information matrix,

say $I_0(\sigma)$, the estimated variance of σ , $R(t)$, or $h(t)$ must be provided first, see Lawless [33]. As a result, the fitted variance of σ (say $\widehat{var}(\hat{\sigma})$) is given by

$$\widehat{var}(\hat{\sigma}) = I_0^{-1}(\hat{\sigma}), \tag{13}$$

where

$$\begin{aligned} I_0(\hat{\sigma}) &= - \left. \frac{d^2 \log L_c(\sigma|\underline{X})}{d\sigma^2} \right|_{\sigma=\hat{\sigma}} \\ &= - \frac{1}{\sigma^2} \left[\frac{3}{2}n - \frac{2}{\sigma} \sum_{i=1}^{J_c} x_i^2 \right] + \frac{2}{\sigma^3} \left[\frac{\xi_c(T_\tau, 4, \sigma)}{\xi_c(T_\tau, 2, \sigma)} + \sum_{i=1}^{J_c} R_i \frac{\xi(x_i, 4, \sigma)}{\xi(x_i, 2, \sigma)} \right] \\ &\quad - \frac{1}{\sigma^4} \left[\left\{ \frac{\xi_c(T_\tau, 6, \sigma)}{\xi_c(T_\tau, 2, \sigma)} - \left(\frac{\xi_c(T_\tau, 4, \sigma)}{\xi_c(T_\tau, 2, \sigma)} \right)^2 \right\} + \sum_{i=1}^{J_c} R_i \left\{ \frac{\xi(x_i, 6, \sigma)}{\xi(x_i, 2, \sigma)} - \left(\frac{\xi(x_i, 4, \sigma)}{\xi(x_i, 2, \sigma)} \right)^2 \right\} \right]. \end{aligned}$$

Consequently, the $100(1 - \rho)\%$ ACI-NA of σ is acquired by

$$\hat{\sigma} \pm z_{\frac{\rho}{2}} \hat{\sigma}_\sigma,$$

where $z_{\frac{\rho}{2}}$ denotes the upper $(\frac{\rho}{2})^{th}$ percentage point of the standard normal distribution.

In addition to creating the $100(1 - \rho)\%$ ACI-NA of $R(t)$ or $h(t)$, following Greene [34], the delta approach is adopted in turn to evaluate the estimated variances $\widehat{var}(\hat{R})$ and $\widehat{var}(\hat{h})$ of $\hat{R}(t)$ and $\hat{h}(t)$, respectively, as

$$\widehat{var}(\hat{R}) \approx [\Psi_R \text{var}(\sigma) \Psi_R^\top] \Big|_{\sigma=\hat{\sigma}} \quad \text{and} \quad \widehat{var}(\hat{h}) \approx [\Psi_h \text{var}(\sigma) \Psi_h^\top] \Big|_{\sigma=\hat{\sigma}},$$

where

$$\begin{aligned} \Psi_R &= \frac{dR(t)}{d\sigma} \\ &= \frac{4}{\sqrt{\pi}\sqrt{\sigma^3}} \left[\xi(t, 4, \sigma) - \frac{3}{2\sigma} \xi(t, 2, \sigma) \right], \\ \text{and} \\ \Psi_h &= \frac{dh(t)}{d\sigma} \\ &= t^2 e^{-\frac{t^2}{\sigma}} \xi^{-1}(t, 2, \sigma) \left[\left(\frac{t}{\sigma} \right)^2 - \xi^{-1}(t, 2, \sigma) \xi(t, 4, \sigma) \right]. \end{aligned}$$

Then, the two-sided $100(1 - \rho)\%$ ACIs of $R(t)$ and $h(t)$, using NA approach, are provided by

$$\hat{R}(t) \pm z_{\frac{\rho}{2}} \sqrt{\widehat{var}(\hat{R})} \quad \text{and} \quad \hat{h}(t) \pm z_{\frac{\rho}{2}} \sqrt{\widehat{var}(\hat{h})},$$

respectively.

Nonetheless, the fundamental disadvantage of the traditional ACI-NA for MLE is that it occasionally yields a negative lower limit for a parameter that accepts positive values. Instead of replacing the negative value of the ACI-NA lower bound with a zero, Meeker and Escobar [35] suggested a log-transformed MLE in order to create the ACI-NL for an unknown parameter whose domain takes positive values. Hence, we construct the two-sided $100(1 - \rho)\%$ ACI-NL of σ , for instance, as

$$\hat{\sigma} \exp\left(\pm z_{\frac{\rho}{2}} \widehat{var}(\hat{\sigma}) \hat{\sigma}^{-1}\right),$$

where, in a similar way, other ACIs of $R(t)$ and $h(t)$ can be easily obtained using the NL approach.

4.2. Bayesian Intervals

This subsection investigates the BCI and HPD interval estimators of σ , $R(t)$ and $h(t)$ using their simulated MCMC iterations. However, first, to create the BCI of σ (as an example), order its MCMC variates $\sigma^{(l)}$ for $l = \mathcal{D}^\bullet + 1, \mathcal{D}^\bullet + 2, \dots, \mathcal{D}$ as

$$\sigma^{(\mathcal{D}^\bullet+1)}, \sigma^{(\mathcal{D}^\bullet+2)}, \dots, \sigma^{(\mathcal{D})},$$

hence, the $100(1 - \varrho)\%$ two limits for the BCI of σ is given by

$$\left(\sigma^{(\mathcal{L}^*)}, \sigma^{(\mathcal{U}^*)}\right),$$

where $\mathcal{L}^* = \bar{\mathcal{D}} \frac{\varrho}{2}$ and $\mathcal{U}^* = \bar{\mathcal{D}} \left(1 - \frac{\varrho}{2}\right)$. In a similar pattern, the $100(1 - \varrho)\%$ BCIs of $R(t)$ and $h(t)$ are developed.

Moreover, using the technique proposed by Chen and Shao [36], the $100(1 - \varrho)\%$ HPD interval estimate of σ (as an example) is provided as

$$\sigma^{(I^*)}, \sigma^{(I^*+(1-\varrho)\bar{\mathcal{D}})},$$

where $I^* = \mathcal{D}^\bullet + 1, \mathcal{D}^\bullet + 2, \dots, \mathcal{D}$ is selected so that

$$\sigma^{(I^*+[(1-\varrho)(\bar{\mathcal{D}})])} - \sigma^{(I^*)} = \min_{1 \leq l \leq \varrho \bar{\mathcal{D}}} \left[\sigma^{(l+[(1-\varrho)\bar{\mathcal{D}}])} - \sigma^{(l)} \right],$$

where $[w]$ stands for the largest integer that is less than (or equal) to w .

5. Numerical Comparisons

This section deals with Monte Carlo simulations, which are performed to test the accuracy of the point and interval estimates of the MB's parameters and its reliability indices, such as RF and HRF, provided in the sections that preceded.

5.1. Simulation Design

The relevant performance of the acquired estimators of σ , $R(t)$ and $h(t)$, through several Monte Carlo simulations, is assessed based on various options of T_i , $i = 1, 2$ (threshold times), n (total experimental items), m (effective sample items) and R (removal fashion). Taking $\sigma (= 0.8, 1.5)$, we repeat the T2GPHC process 1000 times. At $t = 0.5$, the plausible values of $R(t)$ are (0.8907, 0.9536) and of $h(t)$ are (0.6477, 0.2726), for $\sigma (= 0.8, 1.5)$, respectively. Taking also two sets of (T_1, T_2) such as (0.5, 1) and (1.5, 2), two different choices of n and m are considered as $n (= 40, 80)$ while the values of m are taken as failure percentages (FPs) such as $\frac{m}{n} (= 50, 80)\%$ of each n . Also, for given (n, m) , four removal plans R are utilized, namely:

$$S1 : R = (n - m, 0^*(m - 1)),$$

$$S2 : R = \left(0^*\left(\frac{m}{2} - 1\right), n - m, 0^*\left(\frac{m}{2}\right)\right),$$

$$S3 : R = (0^*(m - 1), n - m),$$

$$S4 : R = \left(2^*\left(\frac{m}{2}\right), 0^*\left(\frac{m}{2}\right)\right) \text{ and } (1^*n - m, 0^*2m - n), \text{ for FP} = 50 \text{ and } 80\%, \text{ respectively,}$$

where $0^*(m - 1)$ means 0 is repeated $m - 1$ times.

Once 1000 T2GPHC samples are obtained, by installing 'maxLik' package (by Henningsen and Toomet [30]) in R 4.2.2 software, the maximum likelihood and asymptotic interval estimates (from NA and NL methodologies) of σ , $R(t)$ and $h(t)$ are offered. Following the M-H steps proposed in Section 3, we simulated 12,000 MCMC samples and

ignored the first 2000 iterations as burn-in, in turn evaluating the Bayes estimates as well as their BCI/HPD interval estimates of the same objective parameters. According to the prior mean and prior variance criteria.

Two different sets for the values of prior hyperparameters (a, b) are used: Prior-1: Prior-1:(3.2,5) and Prior-2:(6.4,9) (for $\sigma = 0.8$) as well as Prior-1:(6,5) and Prior-2:(12,9) (for $\sigma = 1.5$). Specifically, the given values of a and b are determined in such a way that the prior average reflects the actual value of σ . After installing the ‘coda’ package (by Plummer et al. [28]) in R 4.2.2 software, the evaluation of Bayes findings is conducted. Recently, these packages have been recommended by Elshahhat and Mohammed [37].

The Brooks-Gelman-Rubin (BGR) diagnostic statistic assesses the convergence of Markovian chains by comparing the variances within and variance across chains for each model parameter. Using this criterion, the posterior distribution is said to have converged if the variance-between-to-within ratio is near one; see Nassar and Elshahhat [38]. However, to examine the convergence of the simulated Markovian draws of σ , the BGR diagnostic plots, when $\sigma(= 0.8, 1.5)$, $(n, m) = (40, 20)$, $(T_1, T_2) = (0.5, 1.5)$, S1 and Prior-1 in both sets of σ (as an example), are shown in Figure 1. It shows that there is no significant difference between the simulated chains, demonstrating that the burn-in sample is large enough to ignore the influence of starting point values. So, the collected Markovian chains have converged well.

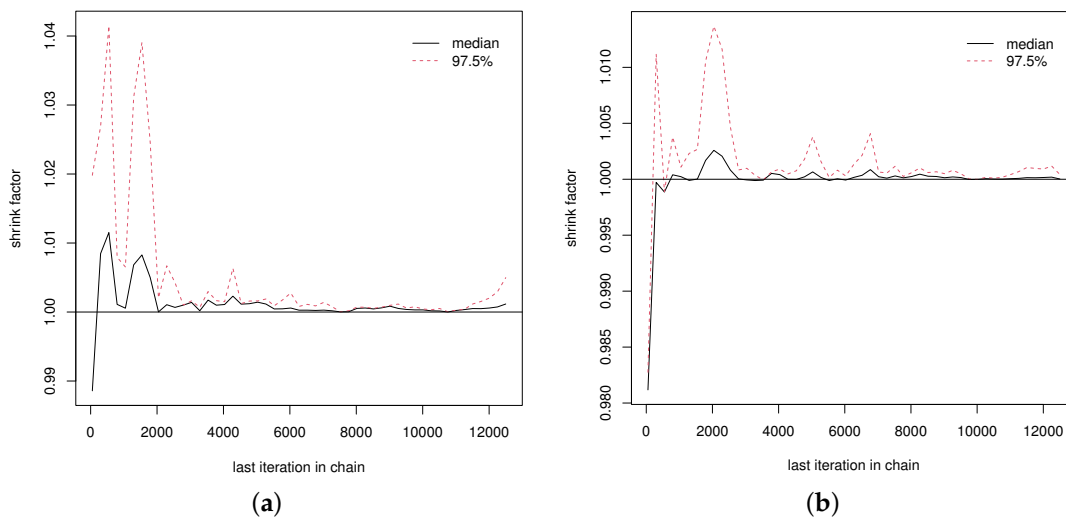


Figure 1. The BGR diagnostic plots for MCMC draws of σ in Monte Carlo simulation. (a) $\sigma = 0.8$; (b) $\sigma = 1.5$.

However, the average point estimates (Av.Es) of σ (for example) are given by

$$\bar{\sigma} = \frac{1}{1000} \sum_{i=1}^{1000} \check{\sigma}^{(i)},$$

where $\check{\sigma}^{(i)}$ is the offered estimate of σ at i th sample.

Comparison between the acquired point estimates of σ is made based on their root mean squared-errors (RMSEs) and mean relative absolute biases (MRABs) as

$$RMSE(\check{\sigma}) = \sqrt{\frac{1}{1000} \sum_{i=1}^{1000} (\check{\sigma}^{(i)} - \sigma)^2},$$

and

$$MRAB(\check{\sigma}) = \frac{1}{1000} \sum_{i=1}^{1000} \frac{1}{\sigma} |\check{\sigma}^{(i)} - \sigma|,$$

respectively.

On the other hand, the comparison between the acquired interval estimates of σ is made based on their average confidence lengths (ACLs) and coverage percentages (CPs) as

$$\text{ACL}_{(1-\varrho)\%}(\sigma) = \frac{1}{1000} \sum_{i=1}^{1000} (\mathcal{U}_{\hat{\sigma}^{(i)}} - \mathcal{L}_{\hat{\sigma}^{(i)}}),$$

and

$$\text{CP}_{(1-\varrho)\%}(\sigma) = \frac{1}{1000} \sum_{i=1}^{1000} \mathbf{q}(\mathcal{L}_{\hat{\sigma}^{(i)}}, \mathcal{U}_{\hat{\sigma}^{(i)}})(\sigma),$$

respectively, where $\mathbf{q}(\cdot)$ is the indicator function, $(\mathcal{L}(\cdot), \mathcal{U}(\cdot))$ represent the (lower-bound, upper-bound) of $(1 - \varrho)\%$ asymptotic (or credible) interval of σ . In a similar pattern, the Av.Es, RMSEs, MRABs, ACLs and CPs of $R(t)$, or $h(t)$ can be easily computed.

5.2. Simulation Discussions

One of the best data visualization tools in \mathcal{R} 4.2.2 software is known as a heat-map. Therefore, all simulated outputs (including: RMSEs, MRABs, ACLs, and CPs) of σ , $R(t)$ or $h(t)$ are displayed graphically, in Figures 2–7, by using the heat-map designer. For specialization, from Figures 2–7, the proposed methods are defined on ‘x-axis’ line, while the proposed censoring setting is defined on ‘y-axis’ line. Each heat-map has several notations for distinguishing, using Prior-1 (for example), such as (i) Bayes estimate referred to as “BE-P1”; (ii) BCI estimate referred to as “BCI-P1”; and (iii) HPD estimate referred to as “HPD-P1”.

These maps illustrate various behaviors and findings related to σ , $R(t)$, and $h(t)$, including their relationships with RMSE, MRAB, ACL, and CP values. Key observations derived from these figures include:

- The obtained estimates for σ , $R(t)$, or $h(t)$ demonstrate good behavior and provide accurate results.
- As n (or FP%) increases, all point and interval estimates for life’s unknown parameters perform satisfactorily. A similar finding is observed when $n - m$ decreases.
- With the increase in T_i , $i = 1, 2$, in most tests of all unknown parameters, the simulated CPs of σ , $R(t)$, and $h(t)$ increase, while the simulated RMSEs, MRABs, and ACLs narrow down.
- The Bayes estimates, developed using the M-H algorithm, outperform the frequentist estimates, as they involve more priority information on the unknown parameters.
- Among the four interval estimation techniques, ACI-NA, ACI-NL, BCI, and HPD, there are observable variations in performance under different conditions and for different parameters.
- MCMC calculations using Prior-2 provide more precise estimates than others for all unknown parameters due to Prior-2’s variance being less than Prior-1’s variance.
- The proposed estimates of σ , $R(t)$, and $h(t)$ perform better using S1 ‘left-censoring’ and S4 ‘uniformly censoring’ than other schemes.
- The Bayes M-H methodology is recommended for evaluating the Maxwell–Boltzmann parameters or its reliability time characteristics when data is produced via a generalized Type-II progressively hybrid strategy.
- These findings, illustrated in detail in the Appendix, provide valuable insights into the reliability of the MB distribution when using the T2GPHC strategy.

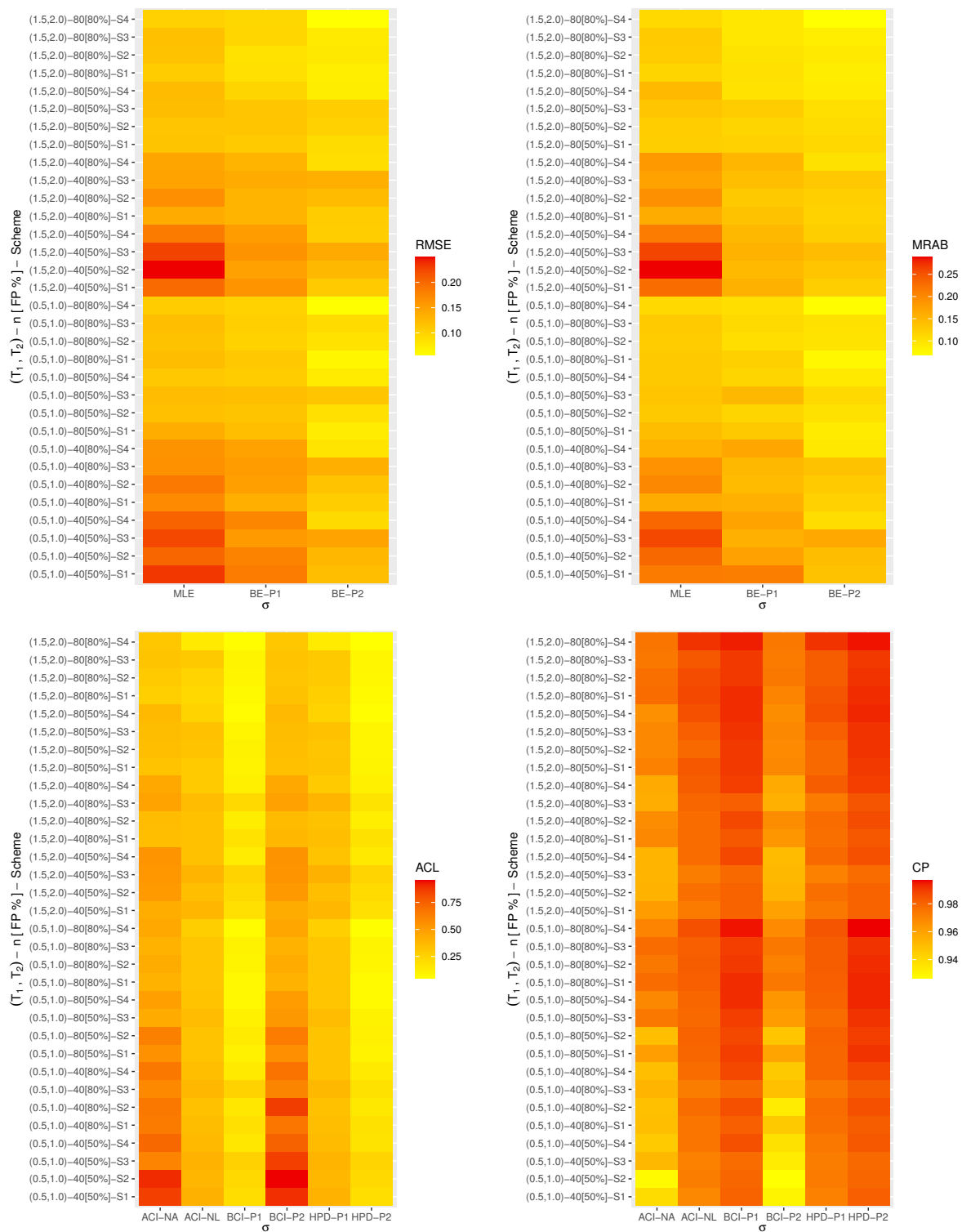


Figure 2. Heat-maps for the Monte Carlo outcomes of σ when $\sigma = 0.8$.

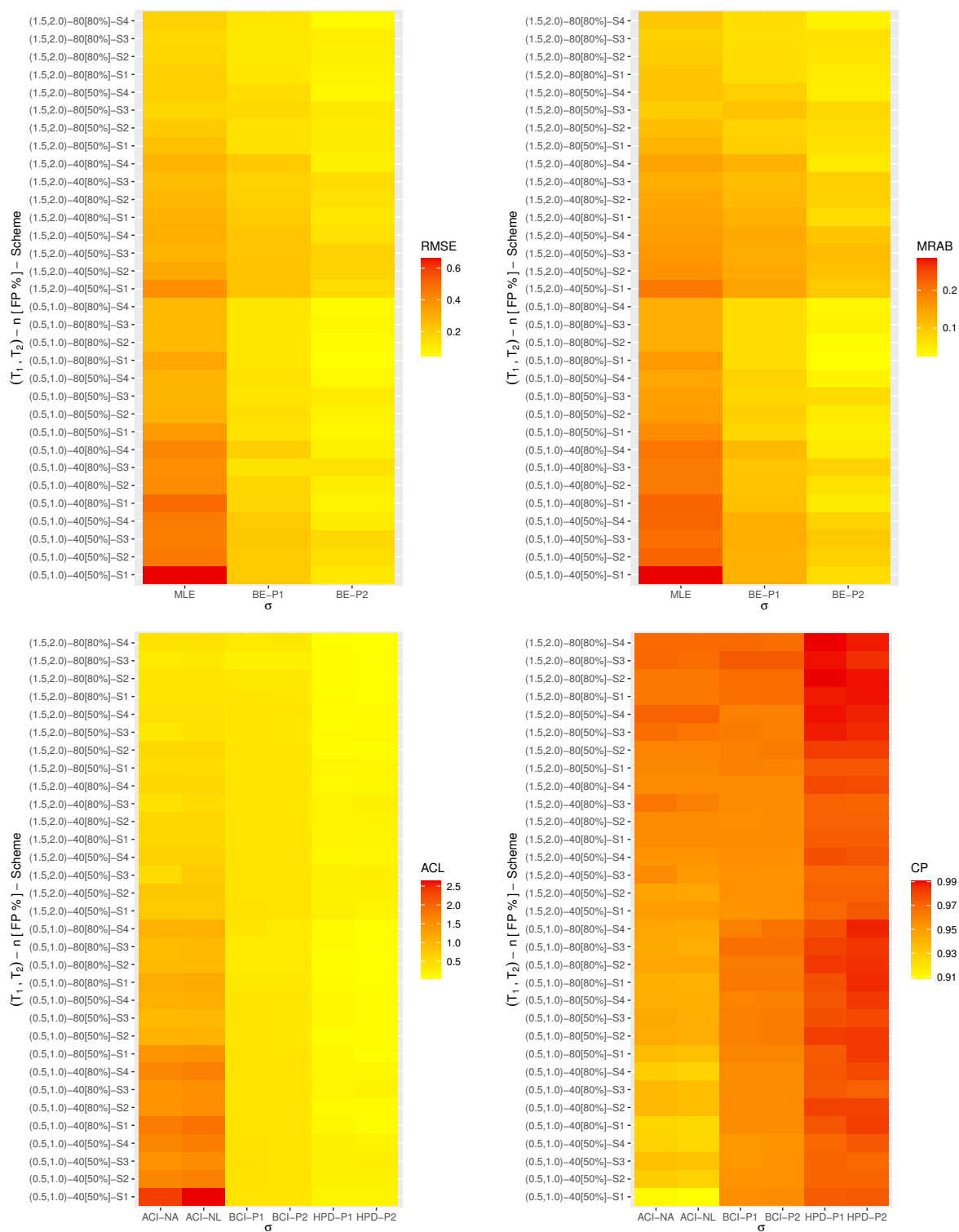


Figure 3. Heat-maps for the Monte Carlo outcomes of σ when $\sigma = 1.5$.

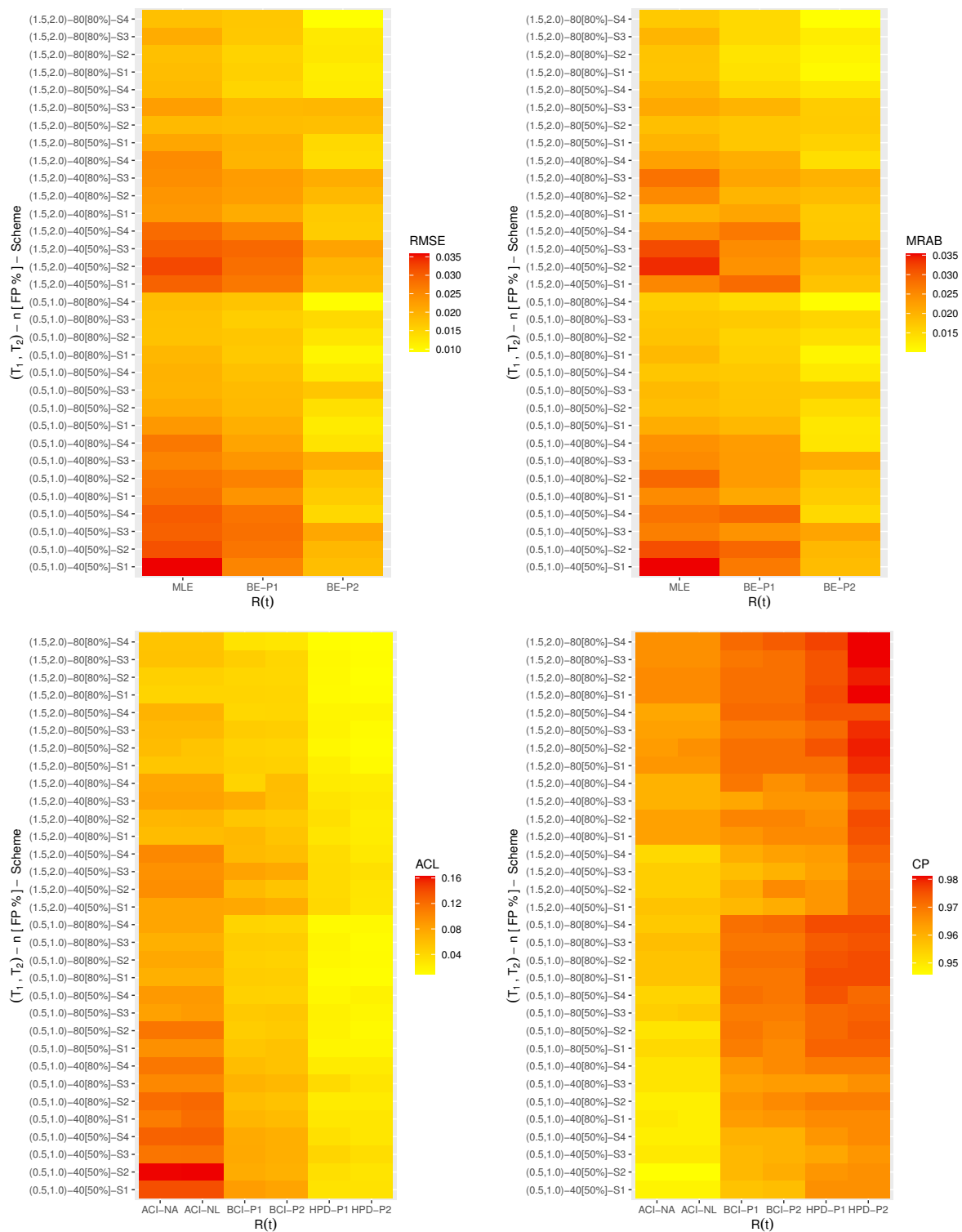


Figure 4. Heat-maps for the Monte Carlo outcomes of $R(t)$ when $\sigma = 0.8$.

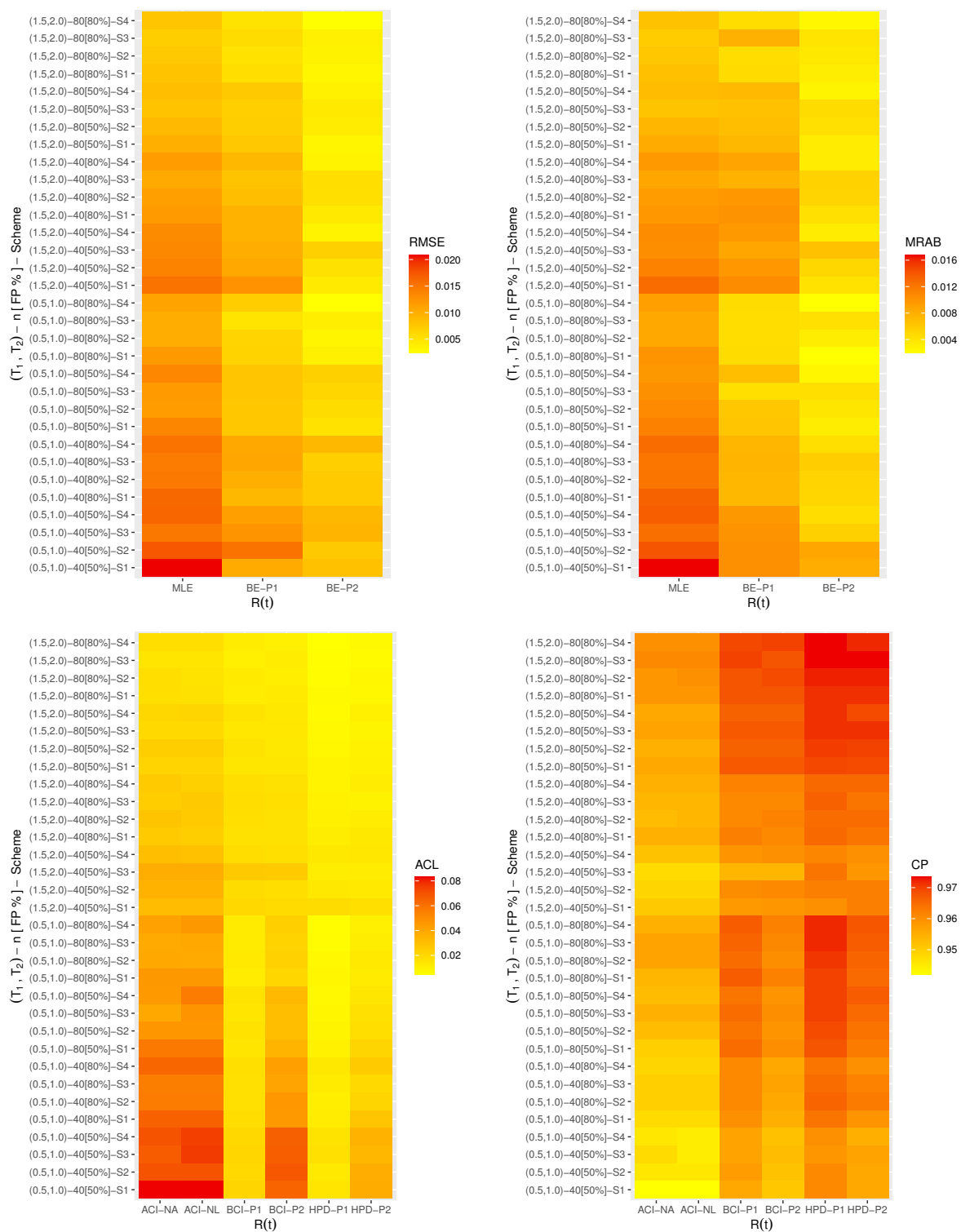


Figure 5. Heat-maps for the Monte Carlo outcomes of $R(t)$ when $\sigma = 1.5$.

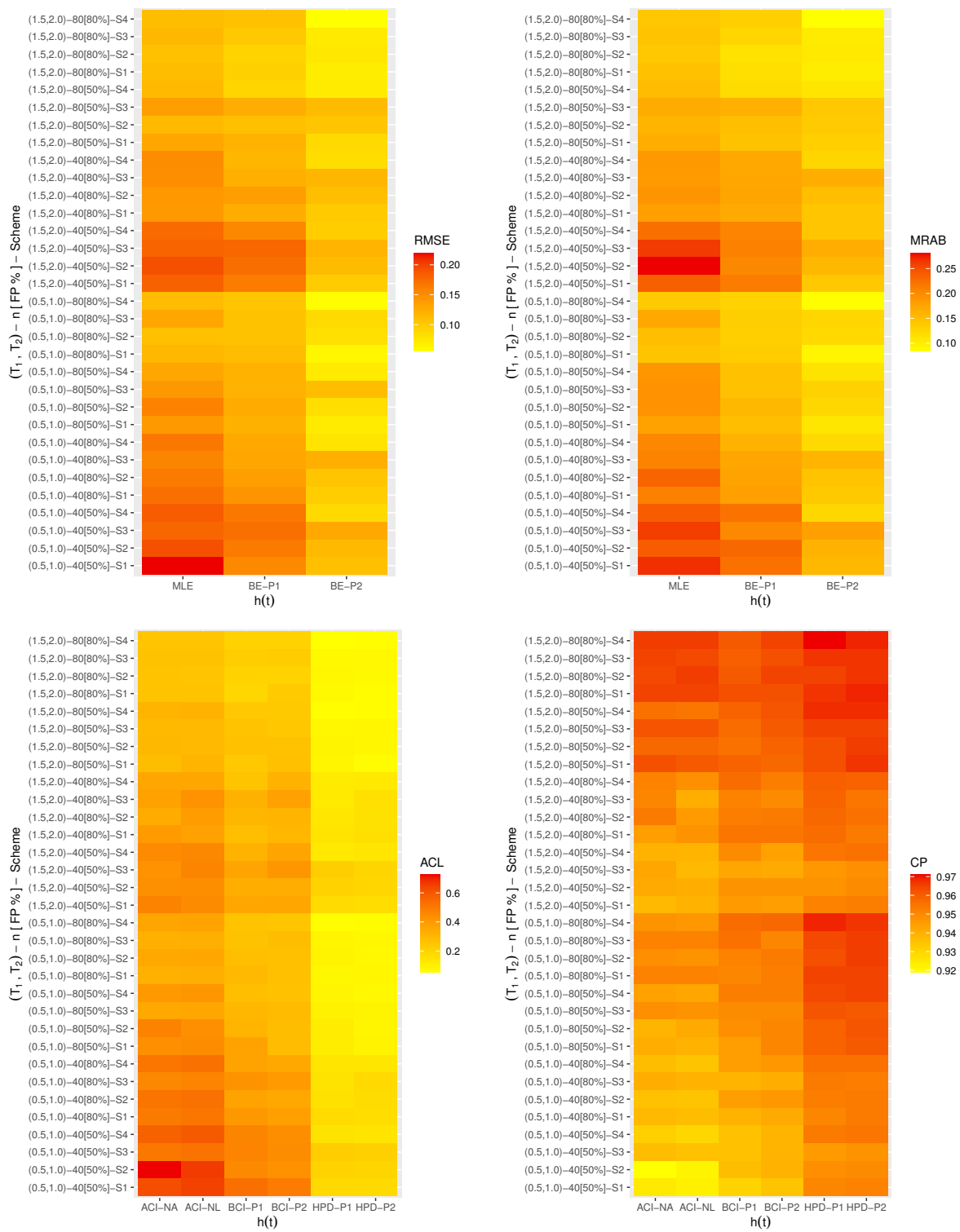


Figure 6. Heat-maps for the Monte Carlo outcomes of $h(t)$ when $\sigma = 0.8$.

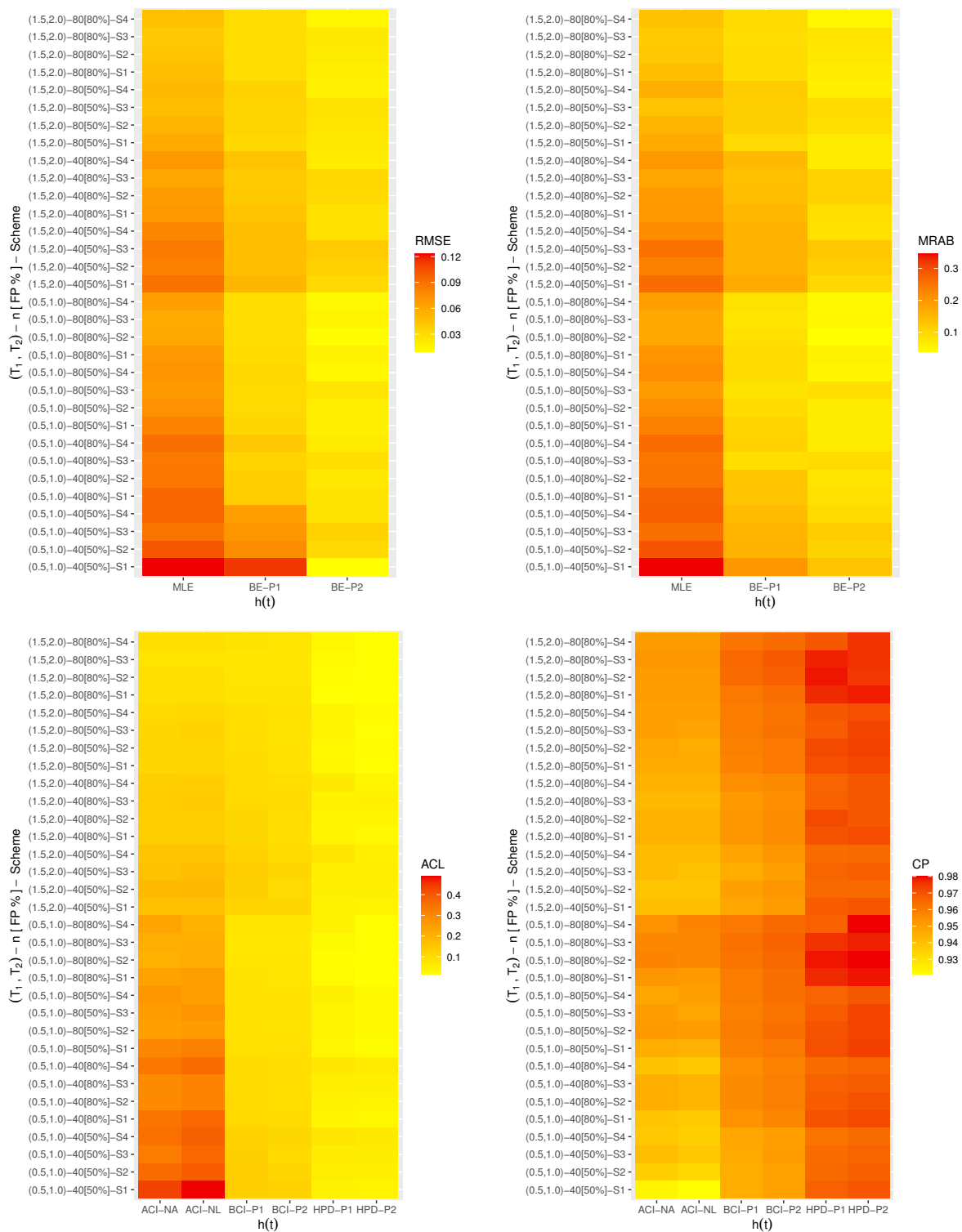


Figure 7. Heat-maps for the Monte Carlo outcomes of $h(t)$ when $\sigma = 1.5$.

6. Real-Life Applications

This section analyses two sets of valuable real data from the engineering and physical sectors to demonstrate the value of the suggested estimating methodologies and the relevance of research objectives to actual scenarios. These examples demonstrated that the proposed inferential procedures operate effectively with real-world data and the recommended censoring scheme.

6.1. Aircraft Windshield

The windscreen of an aircraft is a sophisticated piece of equipment, consisting of multiple layers of material, including a highly tough outer skin with a heated layer just behind it, all laminated under high temperature and pressure. These breakdowns do not cause aircraft damage, but they do require the repair of a windscreen. This application provides an analysis of a data set, reported by Murthy et al. [39] and rediscussed by Alotaibi et al. [40], representing 84 failure time points of aircraft windshields, see Table 2. To demonstrate whether aircraft windshields data fit the MB distribution or not, the Kolmogorov–Smirnov (K-S) statistic (along with its p -value) is obtained. From Table 2, to establish this objective, the MLE $\hat{\sigma}$ (with its standard–error (St.Er)) of σ is 5.1849(0.4619), meanwhile the K-S (p -value) is 0.0661(0.856). This result confirms the fact that the MB lifetime model fits the aircraft windshield data satisfactorily.

Table 2. Failure times of aircraft windshields.

0.040	1.866	2.385	3.443	0.301	1.876	2.481	3.467	0.309	1.899	2.610	3.478
0.557	1.911	2.625	3.578	0.943	1.912	2.632	3.595	1.070	1.914	2.646	3.699
1.124	1.981	2.661	3.779	1.248	2.010	2.688	3.924	1.281	2.038	2.823	4.035
1.281	2.085	2.890	4.121	1.303	2.089	2.902	4.167	1.432	2.097	2.934	4.240
1.480	2.135	2.962	4.255	1.505	2.154	2.964	4.278	1.506	2.190	3.000	4.305
1.568	2.194	3.103	4.376	1.615	2.223	3.114	4.449	1.619	2.224	3.117	4.485
1.652	2.229	3.166	4.570	1.652	2.300	3.344	4.602	1.757	2.324	3.376	4.663

From aircraft windshields data, in turn to examine the proposed estimation methodologies, three T2GPHC samples based on various combinations of R and T_i , $i = 1, 2$ with FP = 50% are created, see Table 3. For specification, in Table 3, three various PT2C scenarios are used to get samples S_i for $i = 1, 2, 3$, as:

- Scheme-S1: $(1 * m)$;
- Scheme-S2: $(2 * (\frac{m}{2}), 0 * (\frac{m}{2}))$;
- Scheme-S3: $(0 * (\frac{m}{2}), 2 * (\frac{m}{2}))$,

respectively.

For each S_i , $i = 1, 2, 3$, the MLEs (along with their St.Ers) and the 95% ACIs (along with their widths) from NA and NL methods of σ , $R(t)$ and $h(t)$ (at $t = 1.5$) are evaluated and reported in Table 4. Because we have no previous knowledge about the MB parameter from the aircraft windshields data, the Bayes estimate is performed under non-informative assumptions, with the hyperparameter values of a and b set to zero. For computational purposes, we have set $a = b = 0.001$. Eliminating the first 10,000 iterations from the full MCMC 50,000 times as burn-in, the Bayes estimates (with their St.Ers) as well as the BCI/HPD interval estimates (with their widths) are evaluated and also provided in Table 4. For each sample, the classical estimates are taken as starting points to carry out the Bayes results. Table 4 shows that the Bayes estimates of σ , $R(t)$ and $h(t)$ behave better, in terms of the smallest St.Er values, than the others. A similar pattern is also noted when comparing the asymptotic (including: ACI-NA/ACI-NL) intervals with the competitively credible (including: BCI/HPD) intervals.

Additionally, from the remaining 40,000 iterations of σ , $R(t)$ and $h(t)$, several properties, including: mean, mode, first-quartile Q_1 , second (or median) quartile Q_2 , third-quartile Q_3 , standard deviation (St.Dv) and skewness (Skew.) are estimated, see Table 5.

Figure 8 depicts the log-likelihood function for all obtained samples S_i , $i = 1, 2, 3$ at varying choices of σ . It reveals the existence and uniqueness of $\hat{\sigma}$. One of the main issues in Bayesian analysis is how to show that the simulated posterior samples converge weakly to the true parameter. So, from S_i , $i = 1, 2, 3$, Figure 9 displays both the density and trace plots of σ , $R(t)$, and $h(t)$. For discrimination, the solid line refers to the Bayes estimate, while the dashed lines refer to the BCI limits. Figure 9 indicates that the MCMC approach converges favorably, and that the recommended size of the burn-in sample is large enough to eliminate the impact of the proposed beginning values. It also supports the same results

listed in Table 5 and shows that the calculated estimates of σ and $h(t)$ are positive-skewed while those associated with $R(t)$ are negative-skewed. Using sample S_1 (as an example) in Table 3, Figure 10 displays the BGR diagnostic plot and shows that there is no significant difference between the acquired Markovian chains. It also indicates that eliminating the first 10,000 iterations as burn-in is enough to discard the influence of initial guess values.

Table 3. Artificial T2GPHC samples from aircraft windshields data.

Sample	$T_1(d_1)$	$T_2(d_2)$	R^*	T^*	Artificial Data
S_1	4.8(43)	5.5(43)	1	4.8	0.040, 0.309, 0.943, 1.124, 1.281, 1.303, 1.480, 1.506, 1.615, 1.652, 1.757, 1.876, 1.911, 1.914, 2.010, 2.085, 2.097, 2.154, 2.194, 2.224, 2.300, 2.385, 2.610, 2.632, 2.661, 2.823, 2.902, 2.962, 3.000, 3.114, 3.166, 3.376, 3.467, 3.578, 3.699, 3.924, 4.121, 4.240, 4.278, 4.376, 4.485, 4.602, 4.663
S_2	2.5(26)	4.6(42)	0	4.485	0.040, 0.557, 0.943, 1.070, 1.281, 1.303, 1.432, 1.506, 1.568, 1.615, 1.619, 1.652, 1.757, 1.866, 1.914, 1.981, 2.010, 2.038, 2.085, 2.089, 2.097, 2.190, 2.194, 2.223, 2.385, 2.481, 2.610, 2.625, 2.646, 2.902, 2.964, 3.000, 3.117, 3.166, 3.443, 3.578, 3.779, 4.240, 4.305, 4.376, 4.449, 4.485
S_3	2.2(28)	3.7(40)	6	3.7	0.040, 0.301, 0.309, 0.557, 0.943, 1.070, 1.124, 1.248, 1.281, 1.281, 1.303, 1.432, 1.480, 1.505, 1.506, 1.568, 1.615, 1.619, 1.652, 1.652, 1.757, 1.866, 1.876, 1.899, 1.911, 1.912, 2.085, 2.154, 2.385, 2.481, 2.610, 2.646, 2.890, 2.962, 3.103, 3.166, 3.376, 3.443, 3.467, 3.595

Table 4. Estimates of σ , $R(t)$ and $h(t)$ from aircraft windshields data.

Sample	Par.	MLE		MCMC		ACI-NA ACI-NL			BCI HPD		
		Est.	SE	Est.	SE	Lower	Upper	Width	Lower	Upper	Width
S_1	σ	9.2860	1.0830	9.2804	0.1963	7.1634	11.409	4.2451	8.8971	9.6642	0.7671
	$R(1.5)$	0.9223	0.0123	0.9221	0.0022	7.3885	11.671	4.2822	8.8997	9.6658	0.7661
	$h(1.5)$	0.1527	0.0204	0.1529	0.0045	0.8981	0.9464	0.0483	0.9176	0.9264	0.0088
S_2	σ	7.8375	0.9622	7.8334	0.1947	0.8984	0.9467	0.0483	0.9177	0.9265	0.0087
	$R(1.5)$	0.9023	0.0160	0.9022	0.0033	0.1128	0.1926	0.0798	0.1445	0.1619	0.0174
	$h(1.5)$	0.1925	0.0253	0.1928	0.0065	0.1176	0.1983	0.0807	0.1444	0.1617	0.0173
S_3	σ	6.0963	0.7473	6.0904	0.1940	0.1430	0.2420	0.0990	0.1804	0.2061	0.0257
	$R(1.5)$	0.8642	0.0214	0.8638	0.0056	0.1488	0.2489	0.1001	0.1799	0.2055	0.0256
	$h(1.5)$	0.2699	0.0307	0.2706	0.0115	4.6316	7.5610	2.9294	5.7121	6.4730	0.7609
						4.7943	7.7520	2.9577	5.7140	6.4743	0.7603
						0.8222	0.9062	0.0841	0.8524	0.8743	0.0220
						0.8232	0.9073	0.0841	0.8528	0.8747	0.0219
						0.2097	0.3301	0.1204	0.2491	0.2943	0.0452
						0.2159	0.3373	0.1214	0.2483	0.2934	0.0451

Table 5. Properties for 40,000 MCMC iterations of σ , $R(t)$ and $h(t)$ from aircraft windshields data.

Sample	Par.	Mean	Mode	Q_1	Q_2	Q_3	St.Dv	Skew.
S_1	σ	9.28038	9.03596	9.14744	9.27976	9.41397	0.19626	-0.01305
	$R(1.5)$	0.92214	0.91933	0.92066	0.92219	0.92369	0.00224	-0.14448
	$h(1.5)$	0.15294	0.14969	0.14986	0.15284	0.15588	0.00445	0.14790
S_2	σ	7.83344	7.61917	7.70182	7.83284	7.96417	0.19464	0.01719
	$R(1.5)$	0.90216	0.89858	0.90002	0.90224	0.90439	0.00325	-0.14971
	$h(1.5)$	0.19279	0.18673	0.18832	0.19263	0.19708	0.00651	0.15563
S_3	σ	6.09041	5.83385	5.95859	6.09008	6.22052	0.19394	0.02101
	$R(1.5)$	0.86384	0.85630	0.86015	0.86402	0.86768	0.00560	-0.18068
	$h(1.5)$	0.27064	0.25270	0.26271	0.27025	0.27822	0.01152	0.19304

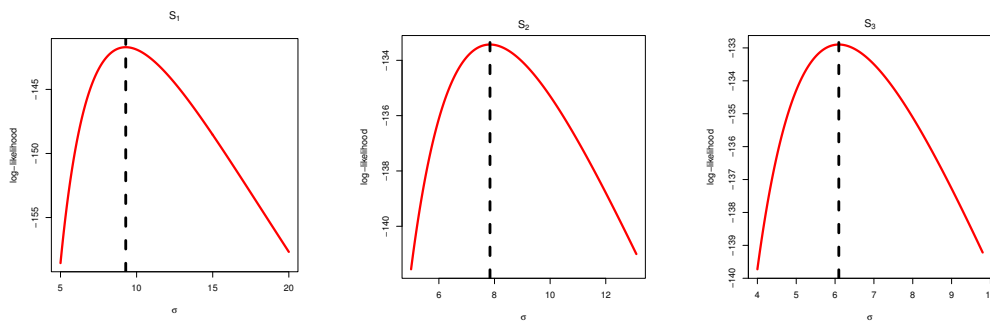


Figure 8. The log-likelihood of σ from aircraft windshields data.

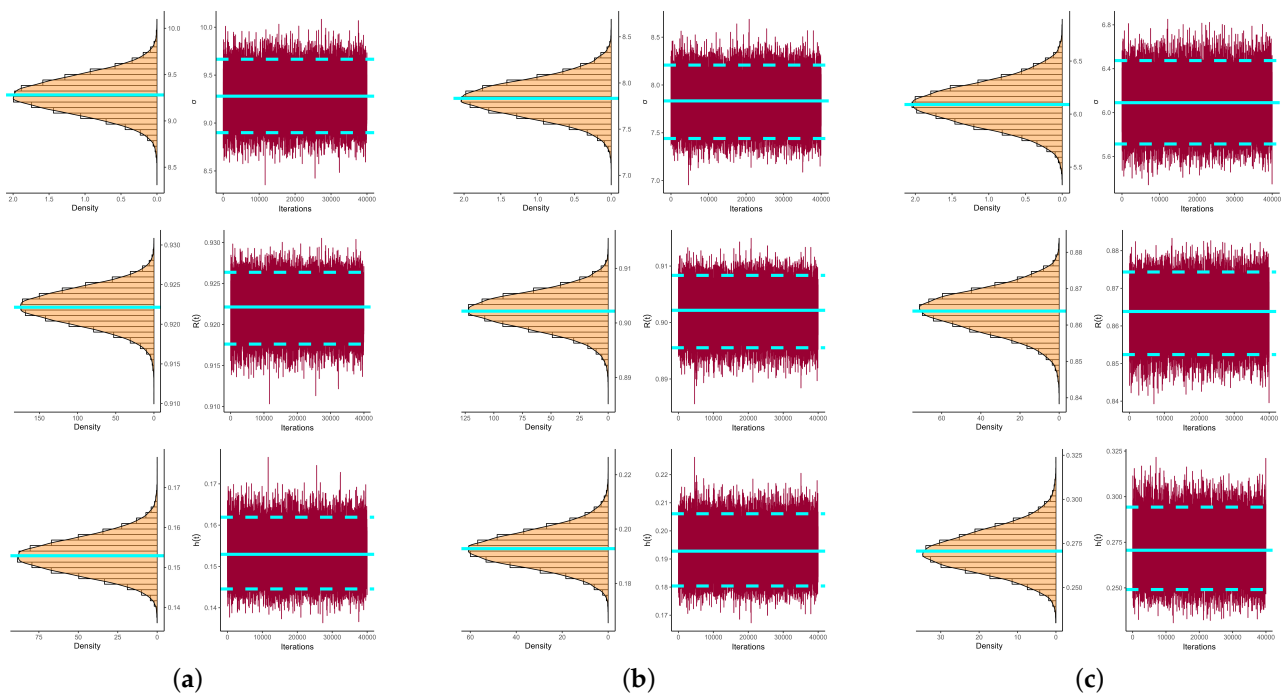


Figure 9. Density (left) and Trace (right) plots of σ , $R(t)$ and $h(t)$ from aircraft windshields data. (a) Sample S_1 ; (b) Sample S_2 ; (c) Sample S_3 .

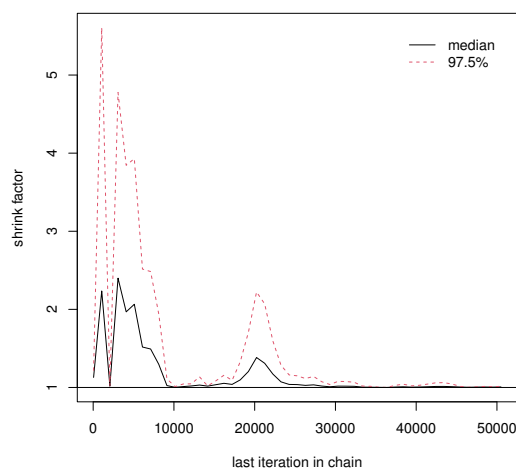


Figure 10. The BGR diagnostic for MCMC draws of σ from aircraft windshields data.

One of the most challenging aspects of reliability inference is determining how to discover the real behavior of the reliability $R(t)$ parameter across all data points. Thus,

in Figure 11, from Table 3, the two bounds of ACI-NA, ACI-NL, BCI and HPD interval estimates are displayed. It demonstrates, in terms of the smallest interval width, that the Bayes (BCI/HPD) interval limits perform superiorly compared to the asymptotic (ACI-NA/ACI-NL) interval limits.

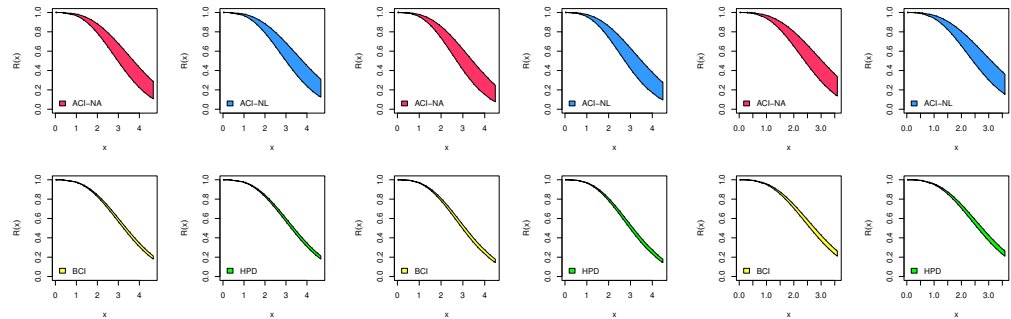


Figure 11. Interval limits of $R(t)$ at all aircraft windshields data points.

6.2. Wind Speed

Wind speed (or wind-flow speed) is a primary atmospheric phenomenon created by air flowing from high-pressure regions to low pressure, often due to temperature variations. The daily average speed of the wind under unpredictability is crucial for forecasting the weather, aircraft and shipping construction, and building engineering. This application analyzes a meteorological data set reflecting the daily average wind speed (AWS) data from 1 January to 10 April 2009, in Cairo, Egypt. This data set was originally taken from Ghazal and Hasaballah [41] and later reanalyzed by Cheema et al. [42]. For calculation convenience, each point in the AWS data is divided by ten. The new transformed sample points for AWS data are shown in Table 6. Using the complete AWS data, the MLE (with its St.Er) of σ is 0.3867(0.0316) and also the K-S (with its p -value) is 0.0775(0.585). This result is evidence that the AWS data set comes from the MB lifetime model.

Table 6. New transformed AWS data points.

0.27	0.31	0.32	0.32	0.33	0.35	0.35	0.38	0.38	0.38
0.42	0.42	0.43	0.43	0.43	0.44	0.45	0.47	0.47	0.48
0.49	0.49	0.49	0.49	0.50	0.50	0.51	0.52	0.52	0.53
0.54	0.54	0.54	0.54	0.55	0.55	0.56	0.56	0.56	0.57
0.57	0.57	0.58	0.58	0.60	0.61	0.63	0.64	0.66	0.67
0.67	0.68	0.68	0.68	0.68	0.69	0.71	0.73	0.73	0.73
0.74	0.75	0.76	0.76	0.77	0.78	0.79	0.80	0.80	0.82
0.82	0.86	0.87	0.88	0.89	0.93	0.93	0.94	0.94	0.94
0.95	0.96	0.98	0.98	0.99	1.00	1.01	1.03	1.06	1.07
1.11	1.13	1.20	1.22	1.24	1.25	1.33	1.38	1.44	1.47

Just like the scenarios examined in Section 6.1, to evaluate our acquired Bayesian and non-Bayesian estimators of σ , $R(t)$, and $h(t)$, different T2GPHC samples from the AWS data are created and provided in Table 7. From Table 7, the offered estimates of δ , θ , $R(t)$, and $h(t)$ (at $t = 0.5$) obtained via maximum likelihood and Bayes estimation methodologies are evaluated, see Table 8. It shows that acquired point and interval estimates derived from the Bayes' paradigm are quite close to those derived from the maximum-likelihood approach. Interval estimates exhibit similar behavior as well. This is a foregone conclusion owing to a lack of further historical data that could be employed, which resulted in no substantial difference between the proposed frequentist and Bayesian estimations.

Table 7. Artificial T2GPHC samples from AWS data.

Sample	$T_1(d_1)$	$T_2(d_2)$	R^*	T^*	Artificial Data
S_1	1.6(51)	1.9(51)	1	1.8	0.27, 0.32, 0.32, 0.33, 0.35, 0.38, 0.38, 0.43, 0.43, 0.43, 0.44, 0.50, 0.51, 0.52, 0.53, 0.54, 0.54, 0.56, 0.56, 0.58, 0.60, 0.61, 0.63, 0.67, 0.67, 0.68, 0.68, 0.68, 0.69, 0.73, 0.73, 0.76, 0.76, 0.80, 0.82, 0.82, 0.86, 0.89, 0.93, 0.94, 0.95, 0.96, 0.98, 0.99, 1.06, 1.07, 1.20, 1.24, 1.33, 1.44, 1.47
S_2	0.9(35)	1.5(50)	0	1.33	0.27, 0.32, 0.32, 0.35, 0.35, 0.38, 0.44, 0.45, 0.48, 0.49, 0.51, 0.52, 0.52, 0.53, 0.54, 0.54, 0.56, 0.56, 0.56, 0.57, 0.58, 0.58, 0.60, 0.61, 0.63, 0.67, 0.68, 0.73, 0.79, 0.80, 0.80, 0.82, 0.87, 0.88, 0.89, 0.93, 0.93, 0.94, 0.94, 0.94, 0.95, 0.96, 1.06, 1.07, 1.11, 1.20, 1.22, 1.24, 1.25, 1.33
S_3	0.6(31)	1.1(48)	6	1.1	0.27, 0.31, 0.32, 0.32, 0.33, 0.35, 0.35, 0.38, 0.38, 0.38, 0.42, 0.42, 0.43, 0.43, 0.43, 0.44, 0.45, 0.47, 0.47, 0.48, 0.49, 0.49, 0.49, 0.49, 0.50, 0.50, 0.52, 0.54, 0.55, 0.55, 0.57, 0.61, 0.66, 0.67, 0.68, 0.71, 0.73, 0.76, 0.80, 0.82, 0.86, 0.87, 0.88, 0.89, 0.93, 0.93, 0.94, 0.96

Table 8. Estimates of σ , $R(t)$ and $h(t)$ from AWS data.

Sample	Par.	MLE		MCMC		ACI-NA ACI-NL			BCI HPD		
		Est.	SE	Est.	SE	Lower	Upper	Width	Lower	Upper	Width
S_1	σ	0.6995	0.0768	0.7045	0.0685	0.5490	0.8501	0.3011	0.5806	0.8478	0.2671
	$R(0.5)$	0.8697	0.0185	0.8692	0.0164	0.5641	0.8675	0.3034	0.5772	0.8434	0.2663
	$h(0.5)$	0.7756	0.0808	0.7793	0.1009	0.8334	0.9060	0.0726	0.8348	0.8988	0.0640
S_2	σ	0.5045	0.0566	0.5076	0.0520	0.8342	0.9068	0.0726	0.8372	0.9005	0.0633
	$R(0.5)$	0.8034	0.0269	0.8024	0.0244	0.6172	0.9339	0.3167	0.5988	0.9930	0.3942
	$h(0.5)$	1.1939	0.0946	1.2024	0.1594	0.6323	0.9512	0.3189	0.5883	0.9779	0.3896
S_3	σ	0.5889	0.0656	0.5941	0.0606	0.3936	0.6154	0.2219	0.4149	0.6180	0.2031
	$R(0.5)$	0.8377	0.0227	0.8373	0.0207	0.4049	0.6286	0.2237	0.4111	0.6120	0.2009
	$h(0.5)$	0.9748	0.0903	0.9783	0.1306	0.7507	0.8561	0.1055	0.7518	0.8473	0.0955
S_3	σ	0.5889	0.0656	0.5941	0.0606	0.7524	0.8579	0.1055	0.7528	0.8480	0.0951
	$R(0.5)$	0.8377	0.0227	0.8373	0.0207	1.0086	1.3793	0.3707	0.9146	1.5374	0.6228
	$h(0.5)$	0.9748	0.0903	0.9783	0.1306	1.0223	1.3945	0.3722	0.8984	1.5174	0.6191
S_3	σ	0.5889	0.0656	0.5941	0.0606	0.4603	0.7174	0.2571	0.4863	0.7215	0.2352
	$R(0.5)$	0.8377	0.0227	0.8373	0.0207	0.4734	0.7326	0.2592	0.4845	0.7174	0.2329
	$h(0.5)$	0.9748	0.0903	0.9783	0.1306	0.7931	0.8823	0.0891	0.7944	0.8748	0.0804
S_3	σ	0.5889	0.0656	0.5941	0.0606	0.7943	0.8835	0.0892	0.7955	0.8755	0.0801
	$R(0.5)$	0.8377	0.0227	0.8373	0.0207	0.7978	1.1518	0.3540	0.7441	1.2522	0.5081
	$h(0.5)$	0.9748	0.0903	0.9783	0.1306	0.8129	1.1689	0.3559	0.7398	1.2456	0.5057

To highlight the existence and uniqueness of $\hat{\sigma}$, Figure 12 displays the log-likelihood function using samples S_i , $i = 1, 2, 3$ from AWS data. It supports the same findings reported in Table 8 and shows that the acquired MLE of σ exists and is unique. Again, using the same characteristics investigated in Table 9, the vital statistics of σ , $R(t)$ and $h(t)$ are also calculated from AWS data and presented in Table 9. Moreover, to examine the converge status of the proposed MCMC process, both density and trace plots of σ , $R(t)$ and $h(t)$ based on samples S_i , $i = 1, 2, 3$ are shown in Figure 13. It shows that the MCMC approach efficiently converges and that the simulated posterior variates of σ and $h(t)$ are positively skewed, while those associated with $R(t)$ are negatively skewed. Using sample S_1 (as an example) in Table 7, Figure 14 demonstrates that eliminating the first 10,000 iterations as burn-in is sufficient to remove the effect of initial estimate values. It also supports the same conclusion drawn from Figure 13. Using each S_i for $i = 1, 2, 3$, Figure 15 displays the two bounds of all acquired interval estimates at significance level 5%. It is evidence that the BCI and HPD interval limits are very close to the asymptotic interval limits obtained by the NA and NL procedures.

Table 9. Properties for 40,000 MCMC iterations of σ , $R(t)$ and $h(t)$ from AWS data.

Sample	Par.	Mean	Mode	Q_1	Q_2	Q_3	St.Dv	Skew.
S_1	σ	0.70445	0.67695	0.65687	0.70079	0.74852	0.06836	0.32082
	$R(0.5)$	0.86922	0.86409	0.85873	0.87003	0.88071	0.01637	-0.31549
	$h(0.5)$	0.77927	0.81031	0.70833	0.77371	0.84346	0.10087	0.35387
S_2	σ	0.50757	0.50121	0.47141	0.50375	0.54113	0.05196	0.37154
	$R(0.5)$	0.80238	0.80184	0.78658	0.80305	0.81964	0.02442	-0.23096
	$h(0.5)$	1.20241	1.18553	1.08945	1.19628	1.30397	0.15917	0.29797
S_3	σ	0.59408	0.57701	0.55152	0.59051	0.63255	0.06037	0.34675
	$R(0.5)$	0.83733	0.83350	0.82384	0.83826	0.85175	0.02065	-0.27257
	$h(0.5)$	0.97825	1.00134	0.88679	0.97127	1.06262	0.13052	0.32378

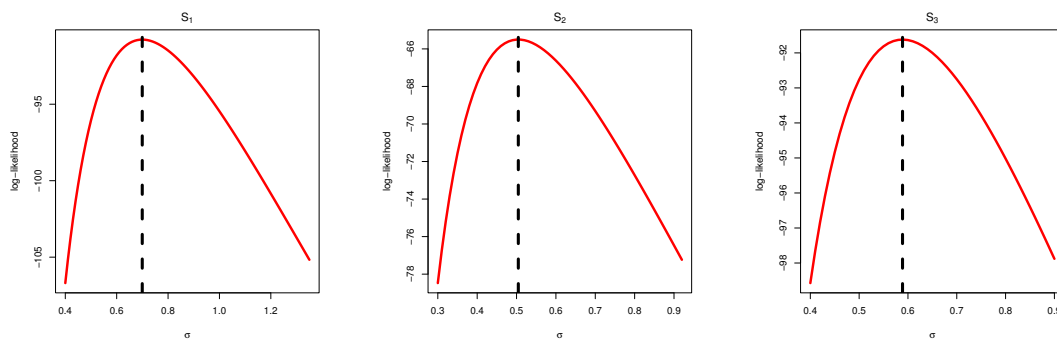


Figure 12. The log-likelihood of σ from AWS data.

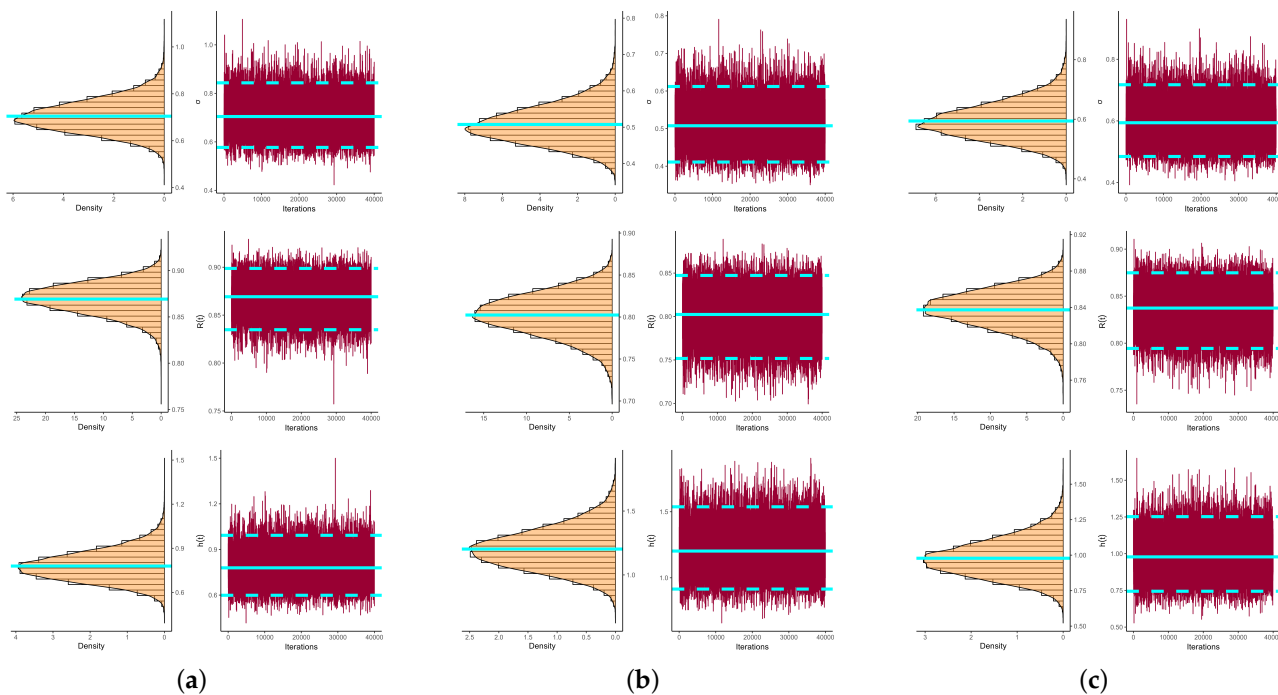


Figure 13. Density (left) and Trace (right) plots of σ , $R(t)$ and $h(t)$ from AWS data. (a) Sample S_1 ; (b) Sample S_2 ; (c) Sample S_3 .

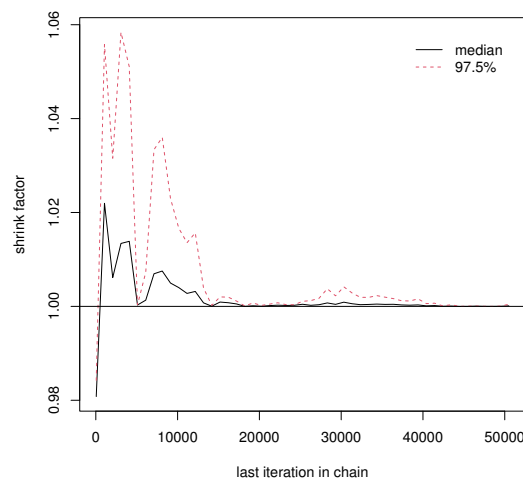


Figure 14. The BGR diagnostic for MCMC draws of σ from AWS data.

Ultimately, based on the proposed engineering and physical applications, we can conclude that the examined methodologies give an appropriate interpretation of the Maxwell–Boltzmann lifespan model when a sample is created by the generalized Type-II progressive hybrid censored process.

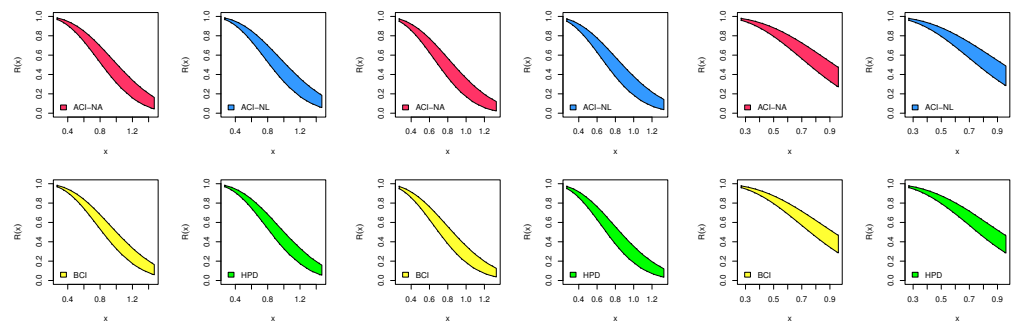


Figure 15. Interval limits of $R(t)$ at all AWS data points.

7. Concluding Remarks

A new extended censoring strategy, which provides the longest duration that the examiner endures to allow the study to run, called the generalized Type-II progressively hybrid process, has been explored in the presence of data collected from the Maxwell–Boltzmann population. Using this sampling strategy, this work takes into account the parametric inference of the unknown model parameter, reliability, and hazard rate functions of the Maxwell–Boltzmann lifetime model. The frequentist and Bayes estimates of the unknown parameters have also been acquired. The asymptotic confidence intervals of the unknown quantities using the asymptotic distribution of the likelihood and log-transformed likelihood estimates have been obtained. Two R programming languages, namely: ‘maxLik’ and ‘coda’ packages, have been used to evaluate the offered maximum likelihood and Bayes estimates, respectively. As we anticipated, because the joint likelihood function has been constructed in complex form, the posterior density function has also been obtained in nonlinear form. As a result, the Metropolis-Hastings approach has been recommended to acquire the Bayesian estimates and accompanying Bayes credible and highest posterior density intervals. Squared-error loss and inverted gamma prior information functions have been considered to produce the Bayes point/interval estimates. To examine the behavior of the provided estimates, several simulation experiments have been performed using various combinations of total test units, observed failure data, thresholds, and progressive censoring strategies. Two examples from the engineering and physics industries, to demonstrate

the utility of the suggested estimating approaches and how the provided estimators may be utilized in practice, have been explored. The Bayes' Metropolis-Hastings paradigm has been recommended for estimating the Maxwell-Boltzmann distribution's parameters, reliability, and hazard functions based on generalized Type-II progressive hybrid censored data. As a future work, one can consider the inferential methodologies suggested in this work for other extended Maxwell models, for example, power Maxwell, Maxwell-Weibull, or alpha power Maxwell distributions, among others. We hope that the findings and techniques given here will be valuable to reliability practitioners and data analysts.

Supplementary Materials: The following supporting information can be downloaded at: <https://www.mdpi.com/article/10.3390/axioms12070618/s1>, Table S1: The Av.Es (1st column), RMSEs (2nd column) and MRABs (3rd column) of σ when $\sigma = 0.8$; Table S2: The Av.Es (1st column), RMSEs (2nd column) and MRABs (3rd column) of σ when $\sigma = 1.5$; Table S3: The Av.Es (1st column), RMSEs (2nd column) and MRABs (3rd column) of $R(t)$ when $\sigma = 0.8$; Table S4: The Av.Es (1st column), RMSEs (2nd column) and MRABs (3rd column) of $R(t)$ when $\sigma = 1.5$; Table S5: The Av.Es (1st column), RMSEs (2nd column) and MRABs (3rd column) of $h(t)$ when $\sigma = 0.8$; Table S6: The Av.Es (1st column), RMSEs (2nd column) and MRABs (3rd column) of $h(t)$ when $\sigma = 1.5$; Table S7: The ACLs (1st column) and CPs (2nd column) of 95% asymptotic and credible intervals of σ when $\sigma = 0.8$; Table S8: The ACLs (1st column) and CPs (2nd column) of 95% asymptotic and credible intervals of σ when $\sigma = 1.5$; Table S9: The ACLs (1st column) and CPs (2nd column) of 95% asymptotic and credible intervals of $R(t)$ when $\sigma = 0.8$; Table S10: The ACLs (1st column) and CPs (2nd column) of 95% asymptotic and credible intervals of $R(t)$ when $\sigma = 1.5$; Table S11: The ACLs (1st column) and CPs (2nd column) of 95% asymptotic and credible intervals of $h(t)$ when $\sigma = 0.8$; Table S12: The ACLs (1st column) and CPs (2nd column) of 95% asymptotic and credible intervals of $h(t)$ when $\sigma = 1.5$.

Author Contributions: Methodology, A.E., O.E.A.-K. and H.S.M.; Funding acquisition, H.S.M.; Software, A.E.; Supervision, H.S.M.; Writing—original draft, A.E. and O.E.A.-K.; Writing—review & editing H.S.M. and O.E.A.-K. All authors have read and agreed to the published version of the manuscript.

Funding: This research was funded by Princess Nourah bint Abdulrahman University Researchers Supporting Project number (PNURSP2023R175), Princess Nourah bint Abdulrahman University, Riyadh, Saudi Arabia.

Data Availability Statement: The authors confirm that the data supporting the findings of this study are available within the article and in Supplementary Materials.

Acknowledgments: The authors would desire to express their gratitude to the editor and the anonymous referees for useful advice and helpful comments. The authors would also like to express their full thanks to Princess Nourah bint Abdulrahman University, Riyadh, Saudi Arabia, for supporting (PNURSP2023R175) this study.

Conflicts of Interest: The authors declare no conflict of interest.

References

1. BahooToroody, F.; Khalaj, S.; Leoni, L.; De Carlo, F.; Di Bona, G.; Forcina, A. Reliability estimation of reinforced slopes to prioritize maintenance actions. *Int. J. Environ. Res. Public Health* **2021**, *18*, 373. [[CrossRef](#)] [[PubMed](#)]
2. Falcone, D.; Di Bona, G.; Duraccio, V.; Silvestri, A. Integrated hazards method (IHM): A new safety allocation technique. In Proceedings of the IASTED International Conference on Modelling and Simulation, Montreal, QC, Canada, 30 May–1 June 2007; pp. 338–343.
3. Balakrishnan, N.; Cramer, E. *The Art of Progressive Censoring*; Springer: Birkhäuser, NY, USA, 2014.
4. Kundu, D.; Joarder, A. Analysis of Type-II progressively hybrid censored data. *Comput. Stat. Data Anal.* **2006**, *50*, 2509–2528. [[CrossRef](#)]
5. Childs, A.; Chandrasekar, B.; Balakrishnan, N. Exact likelihood inference for an exponential parameter under progressive hybrid censoring schemes. In *Statistical Models and Methods for Biomedical and Technical Systems*; Vonta, F., Nikulin, M., Limnios, N., Huber-Carol, C., Eds.; Birkhäuser: Boston, MA, USA, 2008; pp. 319–330.
6. Lee, K.; Sun, H.; Cho, Y. Exact likelihood inference of the exponential parameter under generalized Type II progressive hybrid censoring. *J. Korean Stat. Soc.* **2016**, *45*, 123–136. [[CrossRef](#)]
7. Epstein, B. Truncated life tests in the exponential case. *Ann. Math. Stat.* **1954**, *25*, 555–564. [[CrossRef](#)]

8. Childs, A.; Chandrasekar, B.; Balakrishnan, N.; Kundu, D. Exact likelihood inference based on Type-I and Type-II hybrid censored samples from the exponential distribution. *Ann. Inst. Stat. Math.* **2003**, *55*, 319–330. [[CrossRef](#)]
9. Bain, L.J.; Engelhardt, M. *Statistical Analysis of Reliability and Life-Testing Models*, 2nd ed.; Marcel Dekker: New York, NY, USA, 1991.
10. Ashour, S.; Elshahhat, A. Bayesian and non-Bayesian estimation for Weibull parameters based on generalized Type-II progressive hybrid censoring scheme. *Pak. J. Stat. Oper. Res.* **2016**, *12*, 213–226.
11. Ateya, S.; Mohammed, H. Prediction under Burr-XII distribution based on generalized Type-II progressive hybrid censoring scheme. *J. Egypt. Math. Soc.* **2018**, *26*, 491–508.
12. Seo, J.I. Objective Bayesian analysis for the Weibull distribution with partial information under the generalized Type-II progressive hybrid censoring scheme. *Commun. Stat. Simul. Comput.* **2020**, *51*, 5157–5173. [[CrossRef](#)]
13. Cho, S.; Lee, K. Exact Likelihood Inference for a Competing Risks Model with Generalized Type II Progressive Hybrid Censored Exponential Data. *Symmetry* **2021**, *13*, 887. [[CrossRef](#)]
14. Wang, L.; Zhou, Y.; Lio, Y.; Tripathi, Y.M. Inference for Kumaraswamy Distribution under Generalized Progressive Hybrid Censoring. *Symmetry* **2022**, *14*, 403. [[CrossRef](#)]
15. Nagy, M.; Bakr, M.E.; Alrasheedi, A.F. Analysis with applications of the generalized Type-II progressive hybrid censoring sample from Burr Type-XII model. *Math. Probl. Eng.* **2022**, *2022*, 1241303. [[CrossRef](#)]
16. Alotaibi, R.; Rezk, H.; Elshahhat, A. Computational Analysis for Fréchet Parameters of Life from Generalized Type-II Progressive Hybrid Censored Data with Applications in Physics and Engineering. *Symmetry* **2023**, *15*, 348. [[CrossRef](#)]
17. Elshahhat, A.; Mohammed, H.S.; Abo-Kasem, O.E. Reliability Inferences of the Inverted NH Parameters via Generalized Type-II Progressive Hybrid Censoring with Applications. *Symmetry* **2022**, *14*, 2379. [[CrossRef](#)]
18. Elshahhat, A.; Mohammed, H.S.; Abo-Kasem, O.E. Statistical Evaluations and Applications for IER Parameters from Generalized Progressively Type-II Hybrid Censored Data. *Axioms* **2023**, *12*, 565. [[CrossRef](#)]
19. Peckham, G.D.; McNaught, I.J. Applications of Maxwell-Boltzmann distribution diagrams. *J. Chem. Educ.* **1992**, *69*, 554–558. [[CrossRef](#)]
20. Rowlinson, J.S. The Maxwell–Boltzmann Distribution. *Mol. Phys.* **2005**, *103*, 2821–2828. [[CrossRef](#)]
21. Bekker, A.J.J.; Roux, J.J.J. Reliability characteristics of the Maxwell distribution: A Bayes estimation study. *Commun. Stat. Theory Methods* **2005**, *34*, 2169–2178. [[CrossRef](#)]
22. Krishna, H.; Malik, M. Reliability estimation in Maxwell distribution with Type-II censored data. *Int. J. Qual. Reliab. Manag.* **2009**, *26*, 184–195. [[CrossRef](#)]
23. Krishna, H.; Malik, M. Reliability estimation in Maxwell distribution with progressively Type-II censored data. *J. Stat. Comput. Simul.* **2012**, *82*, 623–641. [[CrossRef](#)]
24. Krishna, H.; Vivekanand; Kumar, K. Estimation in Maxwell distribution with randomly censored data. *J. Stat. Comput. Simul.* **2015**, *85*, 3560–3578. [[CrossRef](#)]
25. Tomer, S.K.; Panwar, M.S. Estimation procedures for Maxwell distribution under Type-I progressive hybrid censoring scheme. *J. Stat. Comput. Simul.* **2015**, *85*, 339–356. [[CrossRef](#)]
26. Chaudhary, S.; Tomer, S.K. Estimation of stress–strength reliability for Maxwell distribution under progressive Type-II censoring scheme. *Int. J. Syst. Assur. Eng. Manag.* **2018**, *9*, 1107–1119. [[CrossRef](#)]
27. Pathak, A.; Kumar, M.; Singh, S.K.; Singh, U.; Tiwari, M.K.; Kumar, S. Bayesian inference for Maxwell Boltzmann distribution on step-stress partially accelerated life test under progressive type-II censoring with binomial removals. *Int. J. Syst. Assur. Eng. Manag.* **2022**, *13*, 1976–2010. [[CrossRef](#)]
28. Plummer, M.; Best, N.; Cowles, K.; Vines, K. CODA: Convergence diagnosis and output analysis for MCMC. *R News* **2006**, *6*, 7–11.
29. Yee, T.W. The VGAM package. *R News* **2008**, *8*, 28–39.
30. Henningsen, A.; Toomet, O. maxLik: A package for maximum likelihood estimation in R. *Comput. Stat.* **2011**, *26*, 443–458. [[CrossRef](#)]
31. Gelman, A.; Carlin, J.B.; Stern, H.S.; Rubin, D.B. *Bayesian Data Analysis*, 2nd ed.; Chapman and Hall/CRC: Boca Raton, FL, USA, 2004.
32. Lynch, S.M. *Introduction to Applied Bayesian Statistics and Estimation for Social Scientists*; Springer: New York, NY USA, 2007.
33. Lawless, J.F. *Statistical Models and Methods for Lifetime Data*, 2nd ed.; John Wiley and Sons: Hoboken, NJ, USA, 2003.
34. Greene, W.H. *Econometric Analysis*, 4th ed.; Prentice-Hall: New York, NY, USA, 2000.
35. Meeker, W.Q.; Escobar, L.A. *Statistical Methods for Reliability Data*; John Wiley and Sons: New York, NY, USA, 2014.
36. Chen, M.H.; Shao, Q.M. Monte Carlo estimation of Bayesian credible and HPD intervals. *J. Comput. Graph. Stat.* **1999**, *8*, 69–92.
37. Elshahhat, A.; Mohammed, H.S. Statistical Analysis and Applications of Adaptive Progressively Type-II Hybrid Poisson–Exponential Censored Data. *Axioms* **2023**, *12*, 533. [[CrossRef](#)]
38. Nassar, M.; Elshahhat, A. Statistical Analysis of Inverse Weibull Constant-Stress Partially Accelerated Life Tests with Adaptive Progressively Type I Censored Data. *Mathematics* **2023**, *11*, 370. [[CrossRef](#)]
39. Murthy, D.P.; Xie, M.; Jiang, R. *Weibull Models*; John Wiley and Sons: New York, NY, USA, 2004.
40. Alotaibi, R.; Okasha, H.; Nassar, M.; Elshahhat, A. A Novel Modified Alpha Power Transformed Weibull Distribution and its Engineering Applications. *Comput. Model. Eng. Sci.* **2023**, *135*, 2065–2089. [[CrossRef](#)]

41. Ghazal, M.G.M.; Hasaballah, H.M. Exponentiated Rayleigh distribution: A Bayes study using MCMC approach based on unified hybrid censored data. *J. Adv. Math.* **2017**, *12*, 6863–6880.
42. Cheema, A.N.; Aslam, M.; Almanjahie, I.M.; Ahmad, I. Mixture modeling of exponentiated pareto distribution in bayesian framework with applications of wind-speed and tensile strength of carbon fiber. *IEEE Access* **2020**, *8*, 178514–178525. [[CrossRef](#)]

Disclaimer/Publisher’s Note: The statements, opinions and data contained in all publications are solely those of the individual author(s) and contributor(s) and not of MDPI and/or the editor(s). MDPI and/or the editor(s) disclaim responsibility for any injury to people or property resulting from any ideas, methods, instructions or products referred to in the content.